CHAPTER-3

Properties of microemulsion with cationic surfactant : effect of PEG-400

3.1 PREVIEW

Microemulsions are thermodynamically stable mixture of water, oil and surfactant[1,2]. One property of a microemulsion is that surfactant sheets separate water and oil domains to microstructured solution. In recent years the effects of biological materials like cholesterol benzoate, sodium deoxycholate and other materials like alcohols and polymers[3-5] in microemulsions have been studied. The knowledge of the structures of microemulsions[6] is important in understanding various physicochemica properties. The different methods used to understand microdroplet dimensions of w/o or o/w type systems have been ultracentrifugation, conductance, viscosity, adiabatic compressibility and time resolved fluorescence etc. The various studies concerning interactions between microemulsion and uncharged water-soluble polymers[7,8] have been reviewed. The interaction between cationic surfactants and uncharged polymers was thought to be very week, if not totally absent. However, the recent papers[5] have shown that such interactions do exist when sufficiently hydrophobic polymers are used. The effect of neutral water-soluble polymers on the physical properties of microemulsion as an aqueous solution has been widely studied; but few studies examine the effect of these polymers in ternary systems at high surfactant and polymer concentrations. Addition of the polymer includes a structural reorganisation of the dispersed water at high surfactant and polymer concentrations. Also, it includes a structural reorganisation of the dispersed water phase such that the droplets grow in size and correspondingly their number density in the microemulsion associate with and become an integral part of the structure of the microemulsion droplets. Also the polymers added to microemulsion form the aggregates[9-14,15]. Surfactants in aromatic solvents, water solubility, droplet size, inter micellar interactions and exchange of materials between droplets as well as the structure and dynamics of this type of microemulsions have been investigated[5]. Studies have been performed of water solubility as a function of the surfactant chain length, the size of the head and the nature of the counterion for a homologous series of surfactants. Also the effect of an oil was investigated by considering aromatic solvents of different physical properties.

The microemulsions occur over a specific part of the ternary phase diagram, the study of which is therefore a prerequisite in the microemulsion research[16].The cationic surfactants are important in many industrial and consumer products[17] e.g. the fabric and hair conditioners, antistatic agents, bactericides etc. Therefore the research in microemulsion, which has cationic surfactant, is important. There are many studies with cationic surfactants[18-21], with anionic surfactants like sodium dodecylsulphate (SDS)[22a,9,23] as well as with non-ionic Brij 35 and Triton X-100. Here we decided to study the properties of a microemulsion containing cetyl trimethylammoniumbromide (CTAB) under similar conditions as was used by us for SDS, Brij 35[22-28] etc. with 1-propanol as cosurfactant. The presence of polymer and surfactant simultaneously in a system is very common. However, the study of polymer influenced microemulsion is spare[22a,10-15]. In this chapter we present the effect of polyethylene glycol (PEG-400) on the titled microemulsion system.

Papoutsi et al.[13] studied the effect of polyethylene glycol of different molecular weights and concentration on the conductance of a microemulsion system consisting of cyclohexane, 1-pentanol, SDS and water. They observed that the microstructure of a microemulsion was affected only when the polyethylene glycol chain was large. In this chapter, we present the results of our studies of phase diagram, conductance, viscosity, optimal salinity etc. of cyclohexane / CTAB / 1-propanol / water system both in the presence and absence of PEG-400 in the temperature of 30-80°C.

3.2 EXPERIMENTAL

The cationic surfactant, cetyl trimethylammoniumbromide (CTAB) was from S.D.Fine Chemicals (India). It was recrystallized thrice from a mixture of acetone and methanol (4:1 v/v). It was dried at 100°C for a few hours before use. The surface tension-concentration profile of aqueous CTAB solution did not show any minimum. 1-propanol (S.D.'s, India) was distilled (b.pt 96.5°C) before use. Cyclohexane (O) was from Merck, India and was used after purification by standard methods[22b]. Doubly distilled water (W) (conductance ~3 x 10^{-6}S cm^{-1} at room temperature) was

used. The electrolytes NaCl, NaBr, NaI, KCl, KBr and KI were of AR grade and were dried before use. The pseudoternary phase diagrams were constructed by using a titration technique described earlier. A Mullard conductivity bridge (UK) was used for conductance measurements. A standardised Ubbelohde viscometer and a calibrated pyknometer were used for viscosity and density measurements respectively. The various properties of single phase microemulsion (i.e. Winsor IV) were studied over a temperature range of 30-80°C. The interfacial tensions (IFT) were determined with the help of a spinning drop tensiometer (University of Texas at Austin, model 500). The surfactant (S) to cosurfactant (CS) concentration ratio was kept at 1:2 (w/w) throughout this work.

3.3 RESULTS AND DISCUSSION

3.3.1 Phase behaviour studies :

The phase diagrams at 30°C of the system in presence of as well as absence of PEG-400 are given in Fig.3 (1-7). In Table 3.1, the percent areas of the phase diagram occupied by the various regions e.g. 1ϕ (L), 2ϕ (L/L) and 2ϕ (S/L) are presented. There is not much effect of the PEG-400 on the phase diagram. Addition of 1% PEG-400 decreased the one phase area by 2.3%. But the areas of L/L and S/L phases increased by ~1.4 and 0.9% respectively. Further addition of PEG-400 did not show any more effect indicating that the area distribution in the phase diagram is independent of PEG-400 concentration. It was observed earlier that the effects of higher concentrations of PEG-1000 and PEG-6000 on the phase diagrams of n-heptane / AOT / water system were negligible[29].

The presence of 1ϕ (L) and 2ϕ (L/L) regions clearly indicate that the interfacial tension (IFT) between oil and water is very low, at least in the first case. PEG-400 does not change the phase areas drastically. This indicates that the IFT is not affected by PEG. PEG is somewhat solvated by water molecules[14,15] and is insoluble in cyclohexane. The very small decrease in 1ϕ area indicates breaking of microemulsion in the presence of PEG, meaning a very small increase in the IFT. However, it is not

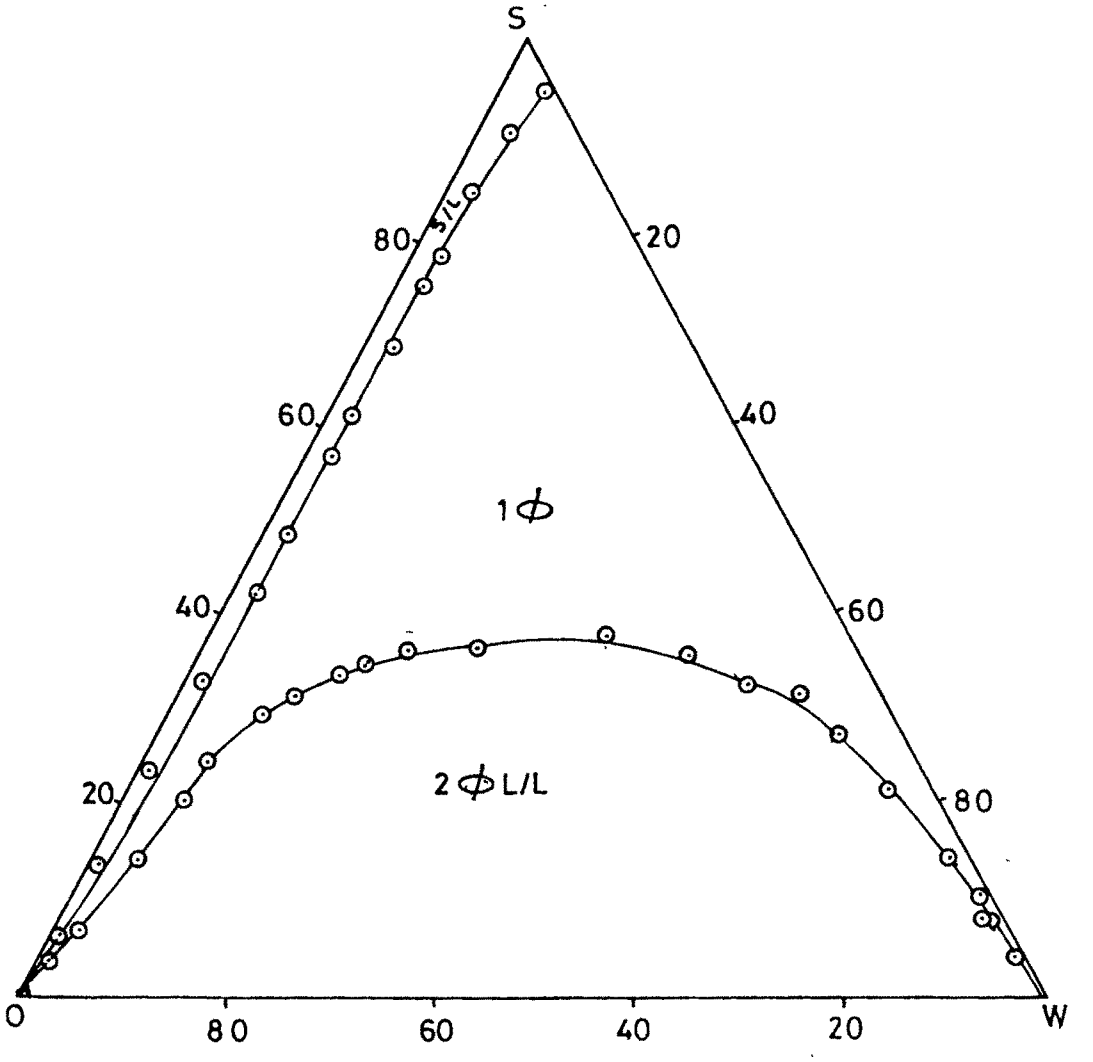

Fig. 3.1 : Pseudoternary phase diagram of the system cyclohexane (O) / CTAB +1-propanol (S) (1:2) / water (W) at 30°C.

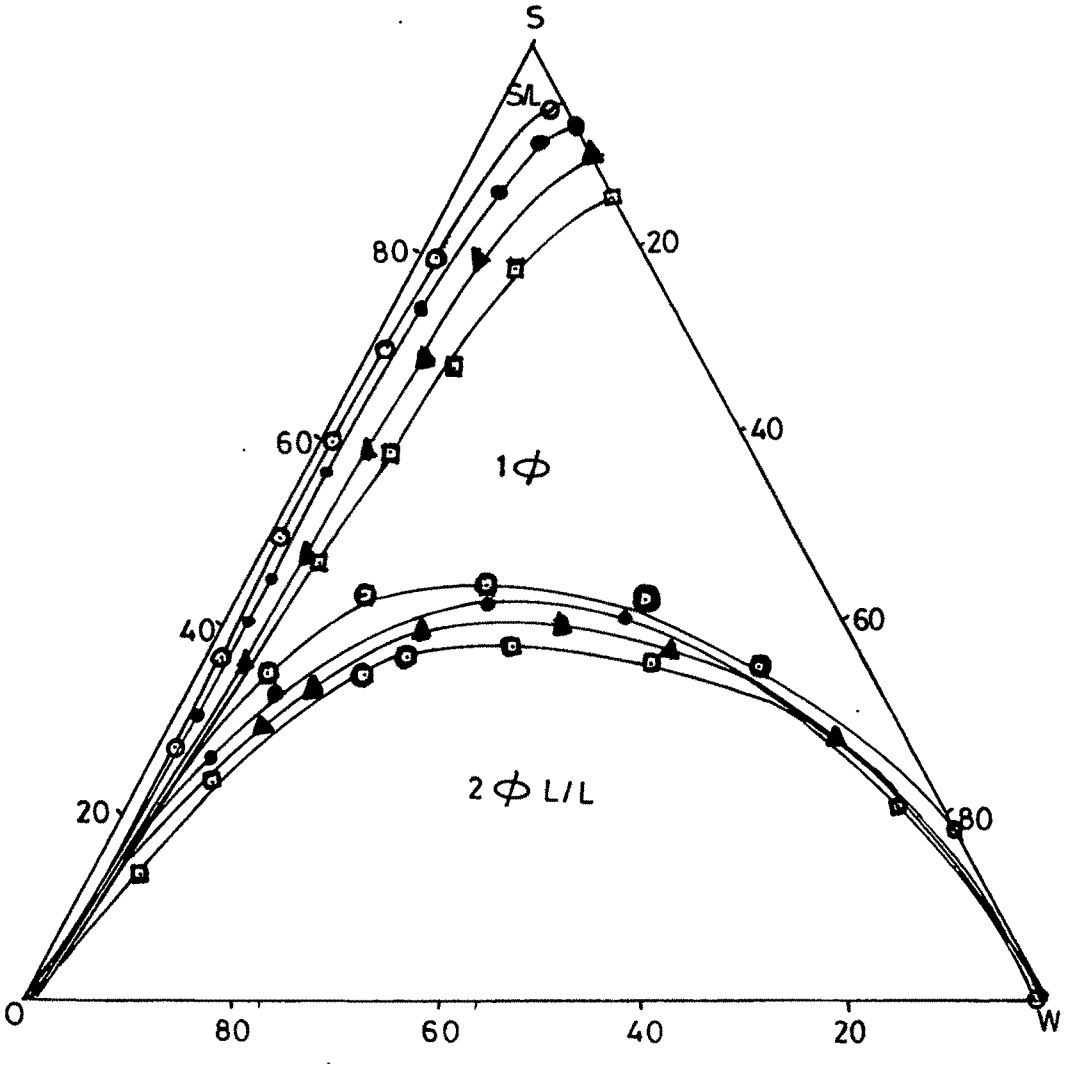

Fig. 3.2 : Pseudoternary phase diagram of the system cyclohexane (O) / CTAB + 1-propanol (S) (1:2) / water (W) at (⊡) 30°C, (▲) 40°C, (●) 50°C, (⊙) 60°C.

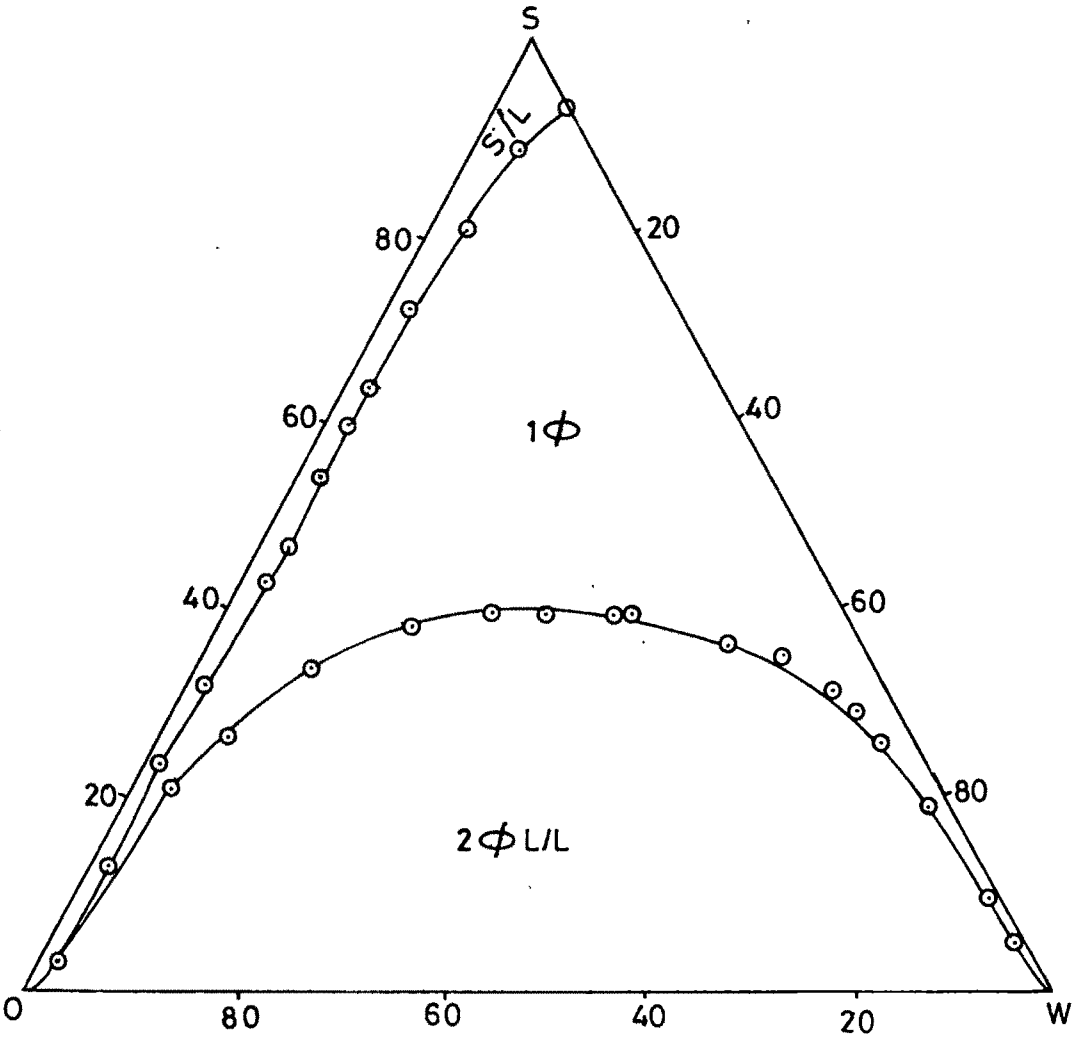

Fig. 3.3 : Pseudoternary phase diagram of the system cyclohexane (O) / CTAB + 1-propanol (S) (1:2) / water (W) with PEG-400 1% w/v at 30°C.

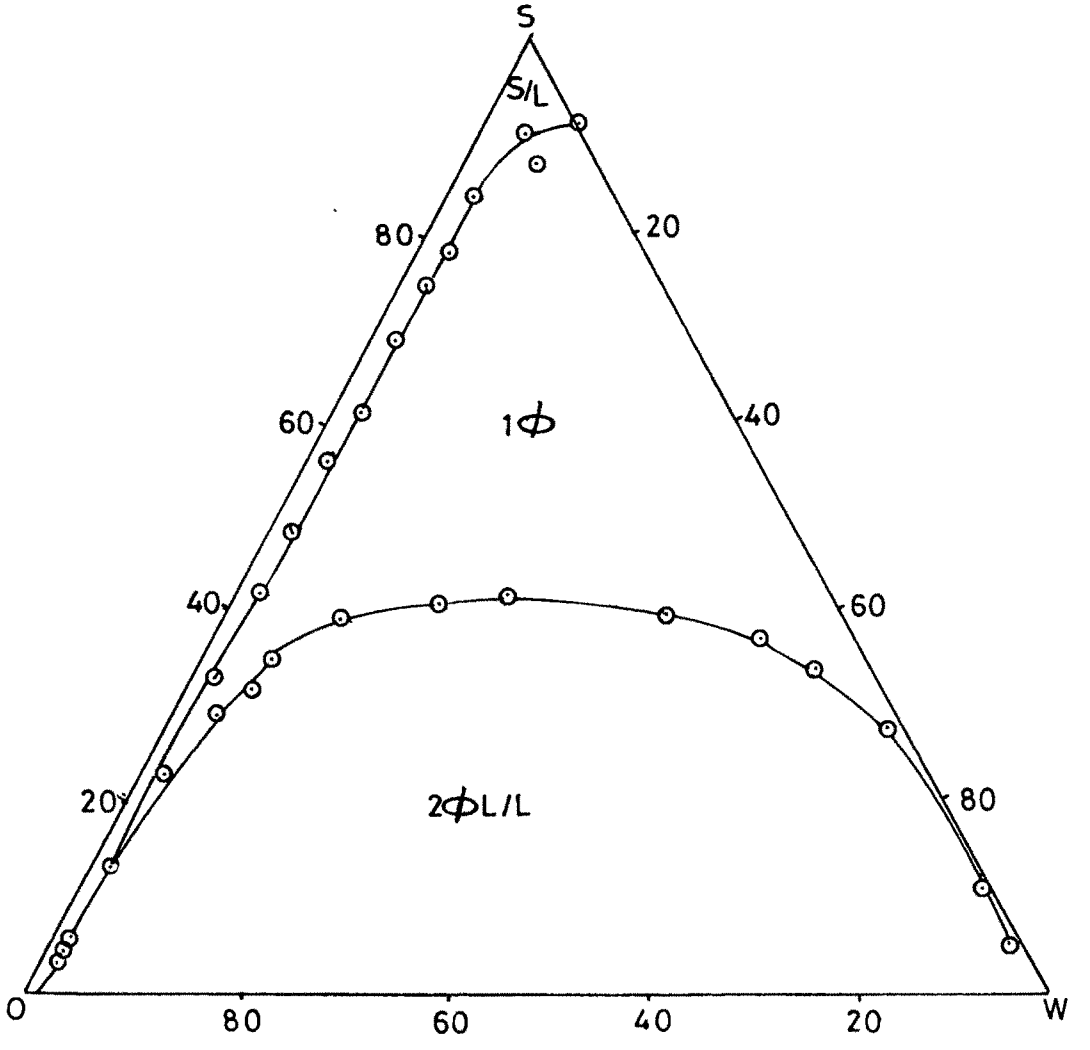

Fig. 3.4 : Pseudoternary phase diagram of the system cyclohexane (O) / CTAB + 1-propanol (S) (1:2) / water (W) with PEG-400 10% w/v at 30°C.

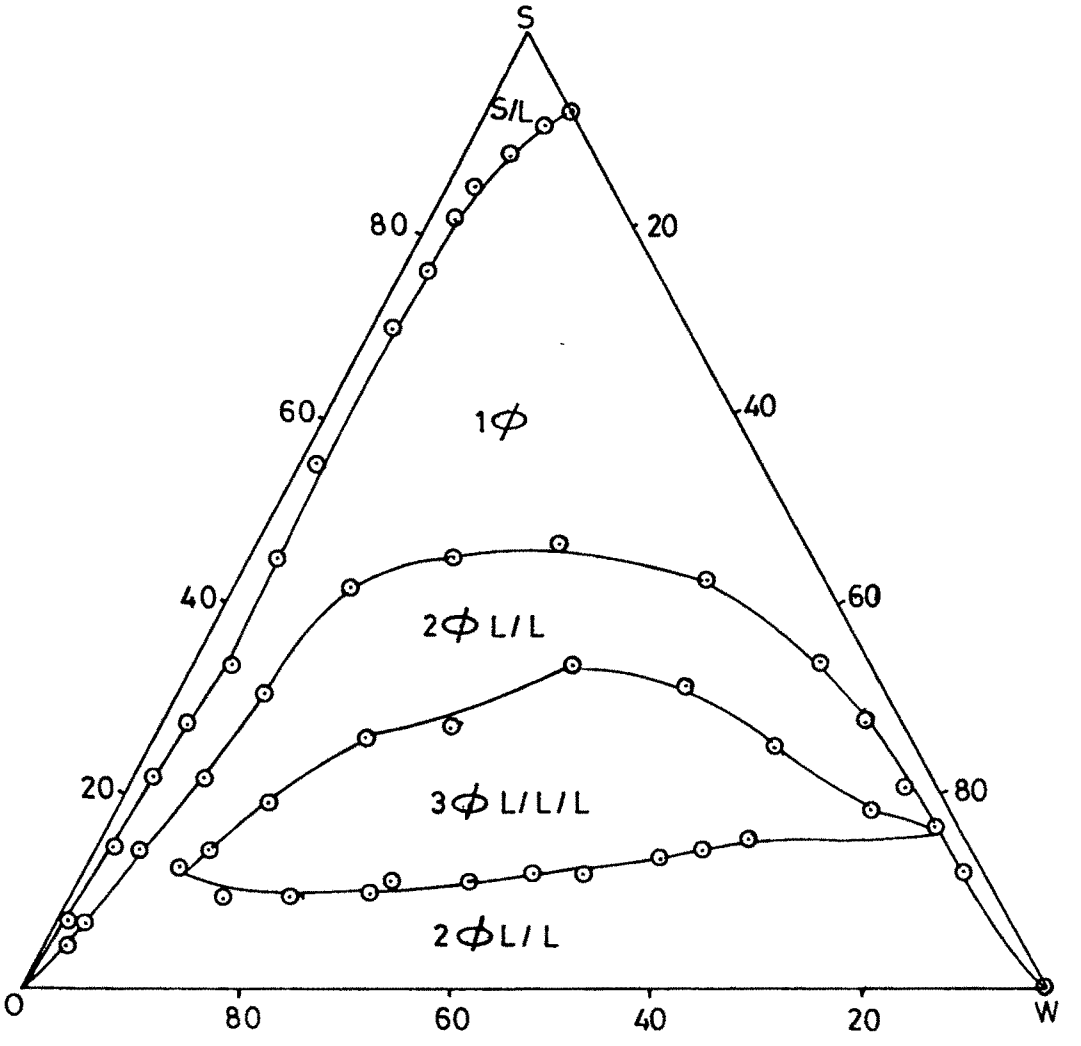

Fig. 3.5 : Pseudoternary phase diagram of cyclohexane (O) / CTAB + 1-propanol (S) (1:2) / water (W) at 40°C.
W = 1M aq. NaCl.

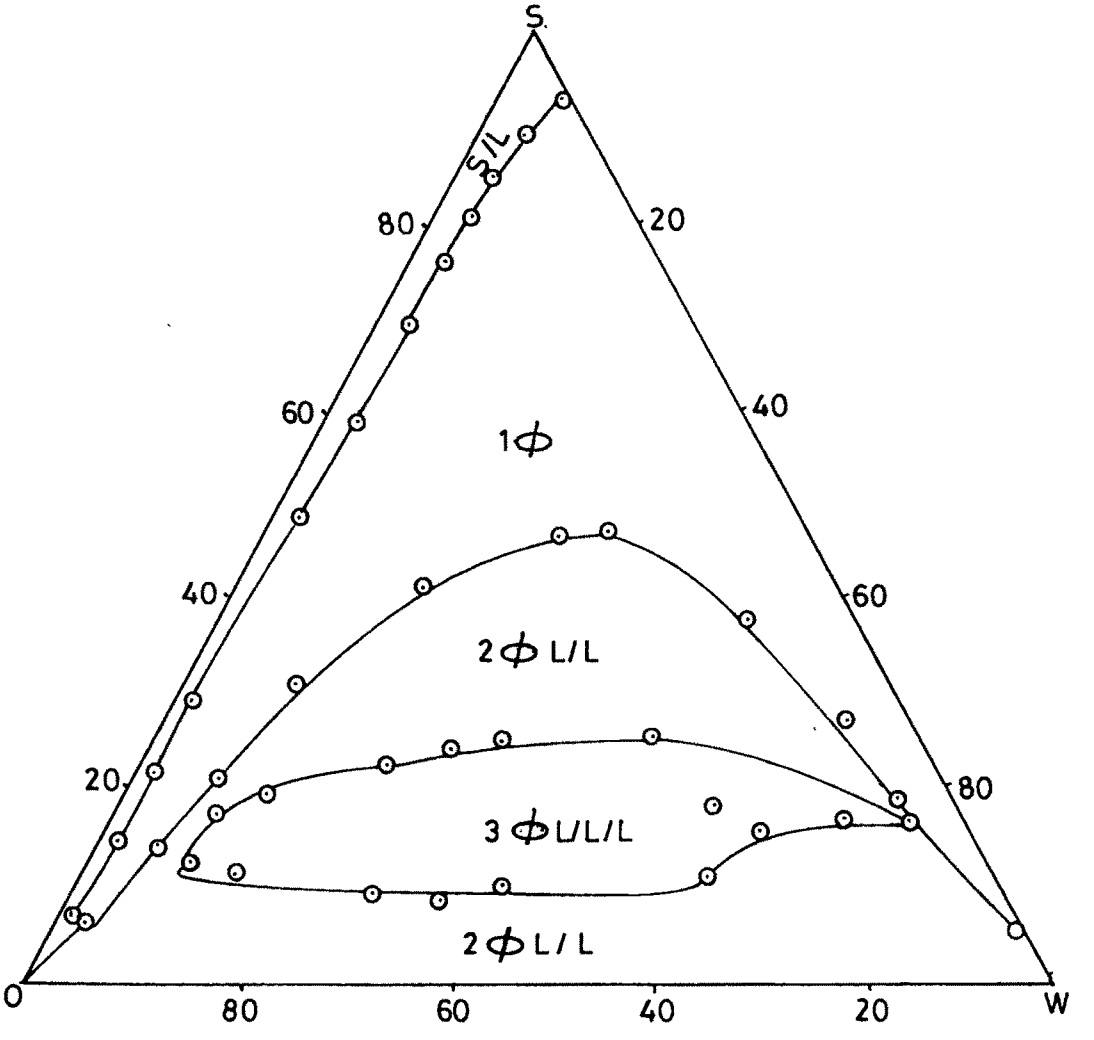

Fig. 3.6 : Pseudoternary phase diagram of the system cyclohexane (O) / CTAB + 1-propanol (S) (1:2) / water (W) at 40°C.
W = 1M aq. NaCl + 10% w/v PEG-400.

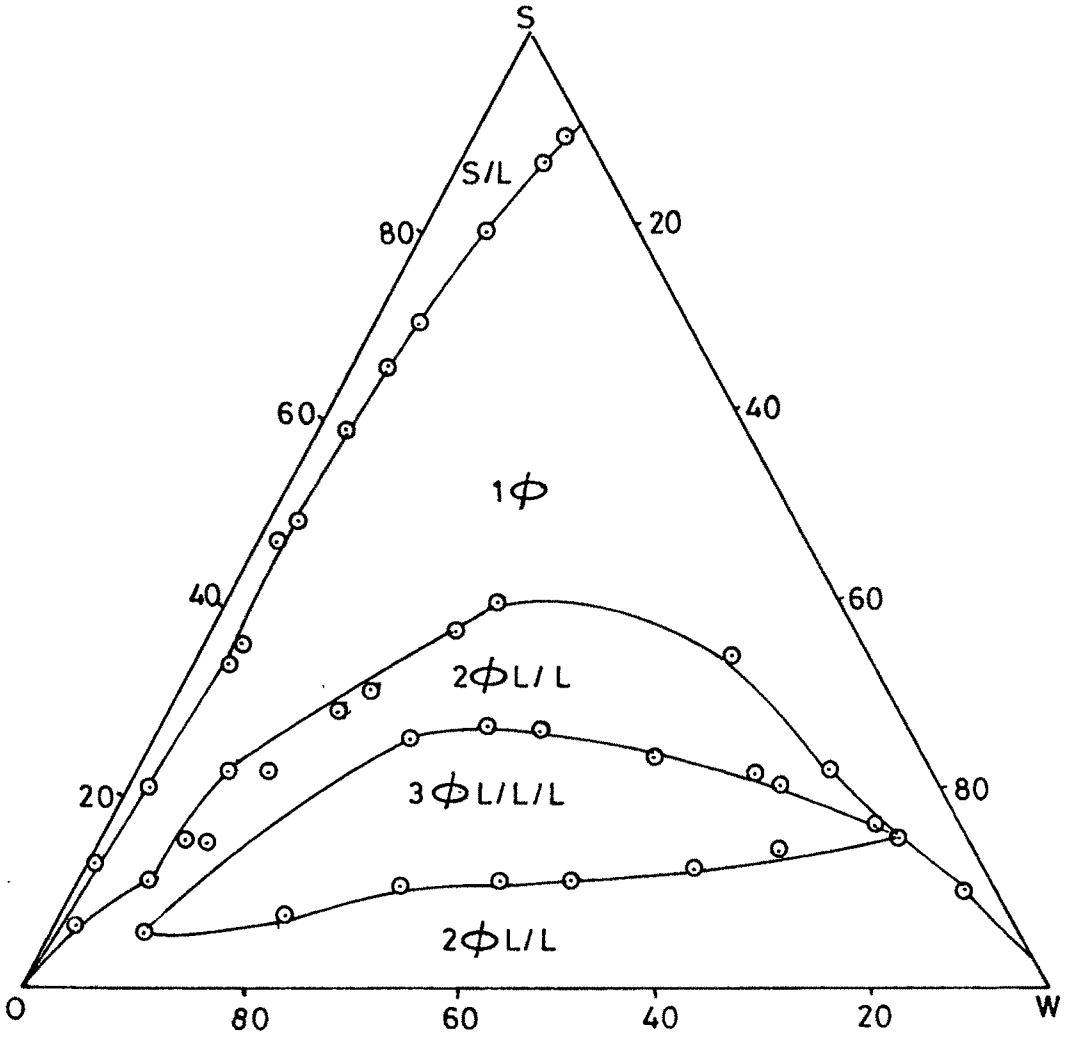

Fig. 3.7 : Pseudoternary phase diagram of the system cyclohexane (O) / CTAB + 1-propanol (S) (1:2) / water (W).
W = 1M aq. NaCl + 20% w/v PEG-400 at 40°C.

possible to prove the statement in the case of 1ϕ region. The 2ϕ (S/L) region increases by 0.9% which is within the experimental error. The phase diagrams were found to change when water was replaced by 1M aqueous NaCl solution [Fig. 3 (5-7)]. In this case a three phase area at the cost of L and L/L regions was obtained (Table 3.1). Presence of PEG-400 increases the three phase areas and decreases the one phase area. One should also note from Fig. 3 (5-7) that the one phase, two phase and three phase regions join at a point in the phase diagram.

3.3.2 **Interfacial tension measurement :**

IFT studies shows that the increase in 3 phase areas by the addition of PEG-400 points towards the increase in IFT between cyclohexane (O) and microemulsion (M) as well as between W and M which is shown in Fig. 3.8. It is obvious here that as water volume increases, the IFT tends towards a constancy. The IFT at W/M interface is somewhat larger than at O/M interface but by only about 0.1 mN m^{-1}. In presence of PEG-400, the interface becomes relatively more unlike water. Also are shown the IFT of CTAB / cyclohexane / 1-propanol at 30°C as a function of CTAB is shown in Fig.3.9. Where as Fig.3.10, 3.11 as well as Fig.3.12 show that the IFT between O/M and W/M in presence of $NaNO_3$, $Ca(NO_3)_2$ as well as $MgCl_2$ as a function of salt concentration, where cyclohexane O = 42.5% S+CS = 17.5% and W = 40%.

3.3.3 **Volume measurement study :**

In Fig. 3 (13-15) are the representative curves for the transition from Winsor type I (WI) to WII via WIII are shown when salts were added to a system of composition 0 = 42.5%, S+CS = 17.5% and W = 40%. The transitions are similar to what was observed in systems with SDS[9] though the concentrations at which WIII forms are considerably lower. Various alkali halides were used in this case and it was observed that the initiation of the three phase system is at lower concentration as the halide component of the salt is changed from $Cl^- \rightarrow Br^- \rightarrow I^-$ though the change of cation

Table 3.1 : Percentage phase regions in the pseudoternary phase diagram of cyclohexane / CTAB / 1-propanol / X system at 30 and 40°C.

X =	Water				1% PEG	10% PEG	1M NaCl	1M NaCl + 10% PEG	1M NaCl + 20% PEG
.	30	40	50	60	30	30	40	40	40°C
1ϕ (L)	45.2	41.10	36.10	35.70	46.9	46.5	41.3	40.0	37.9
2ϕ (L/L)	49.30	53.80	59.20	60.2	46.9	47.2	39.4	36.6	35.4
2ϕ (S/L)	5.40	5.05	4.60	4.0	6.2	6.3	5.9	6.8	7.4
3ϕ (L/L/L)	--	--	--	--	--	--	13.4	16.6	19.3

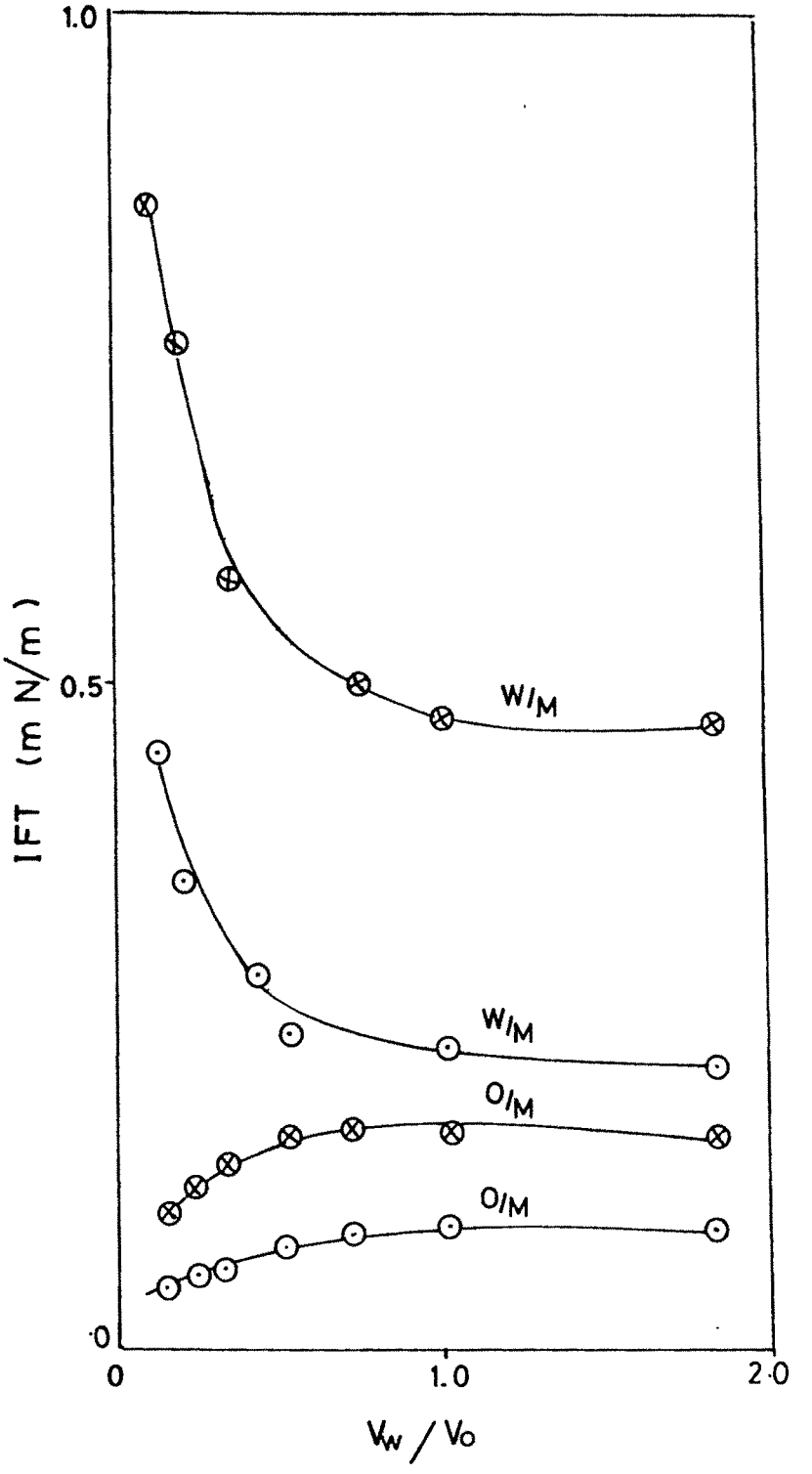

Fig. 3.8 : The variation of interfacial tension (IFT) as a function of water / oil volume ratio at 40°C, S + CS = 22.5%, ⊙ - without PEG-400; ⊗ - with PEG-400.

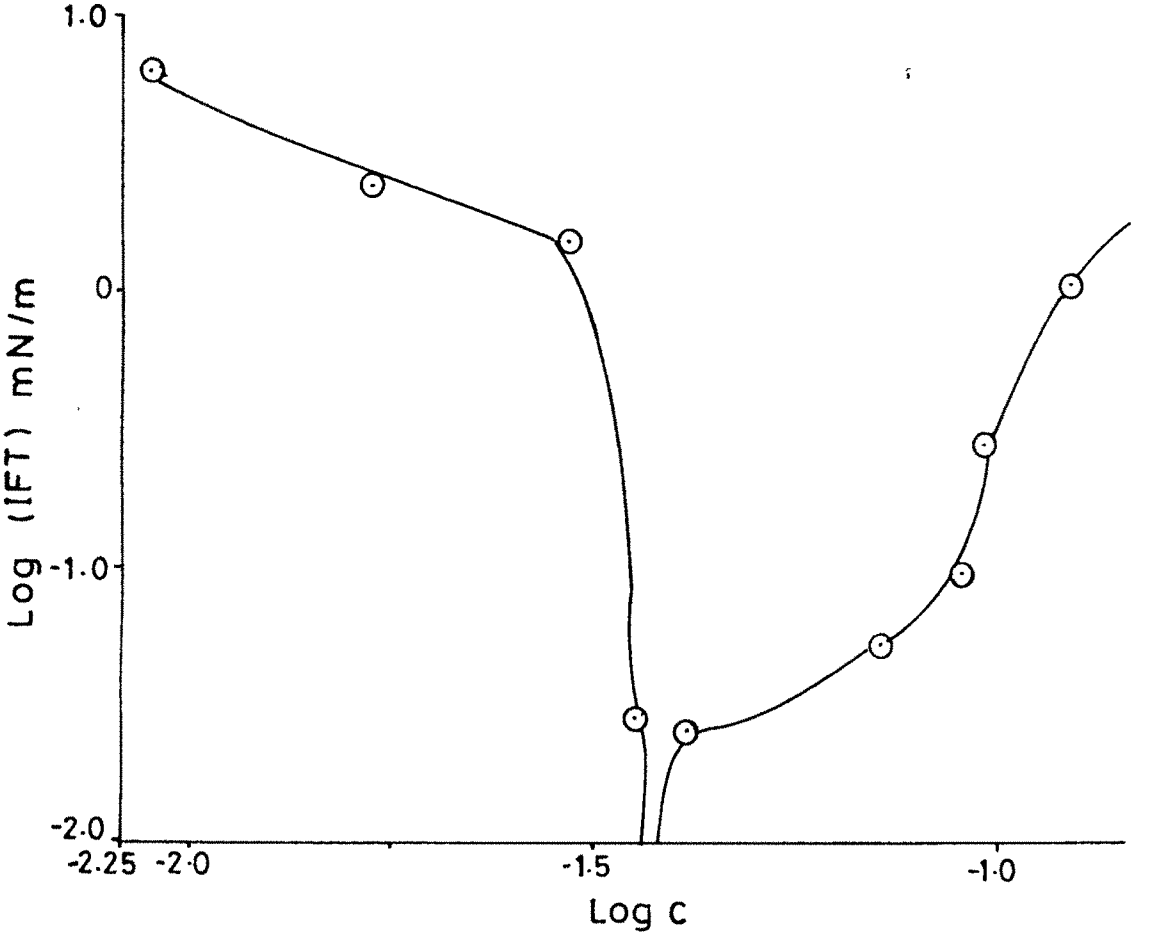

Fig. 3.9 : Plot of interfacial tension (IFT) as a function of concentration (C) of CTAB in (mol / dm^3) at 40°C.

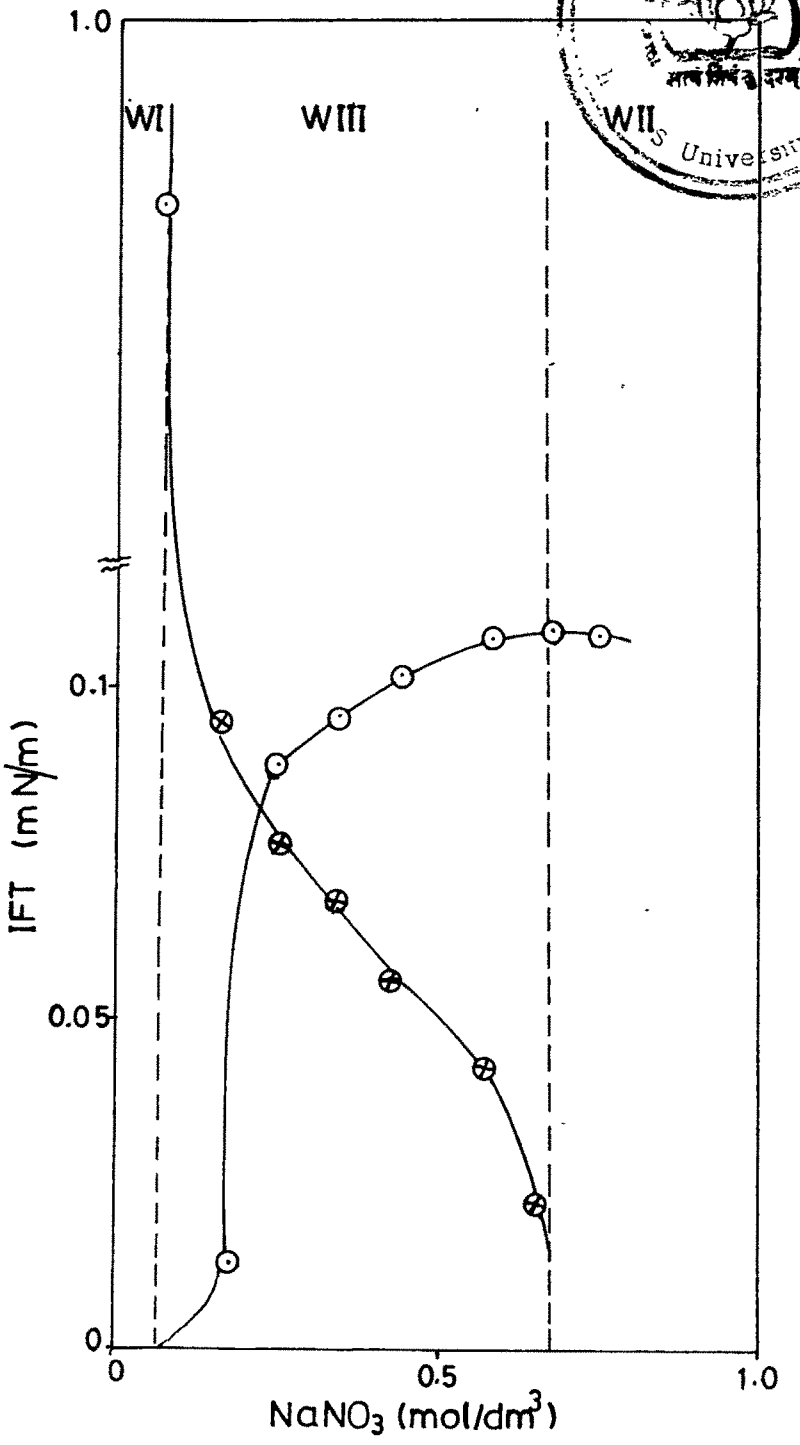

Fig. 3.10 : Plot of variation of interfacial tension (IFT) as function of concentration of $NaNO_3$ (mol / dm^3) between O/M ⊗, between W/M ⊙.

O = 42.5%; W = 40%; S+CS = 17.5% at 35°C.

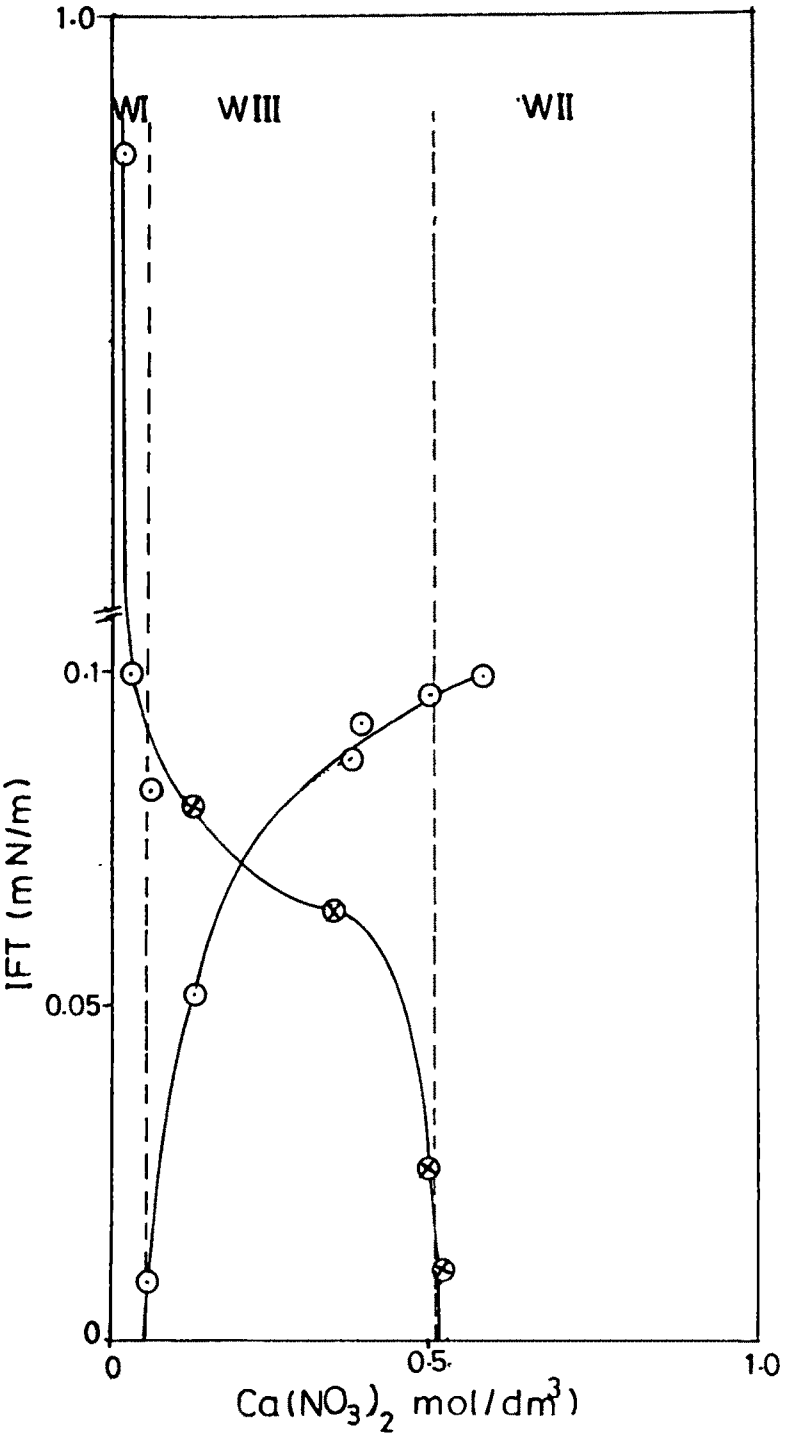

Fig. 3.11 : Plot of variation of interfacial tension (IFT) as a function of concentration of $Ca(NO_3)_2$ (mol / dm^3) between O/M ⊗, between W/M ⊙.

O = 42.4%; W = 40%; S+CS = 17.5% at 35°C.

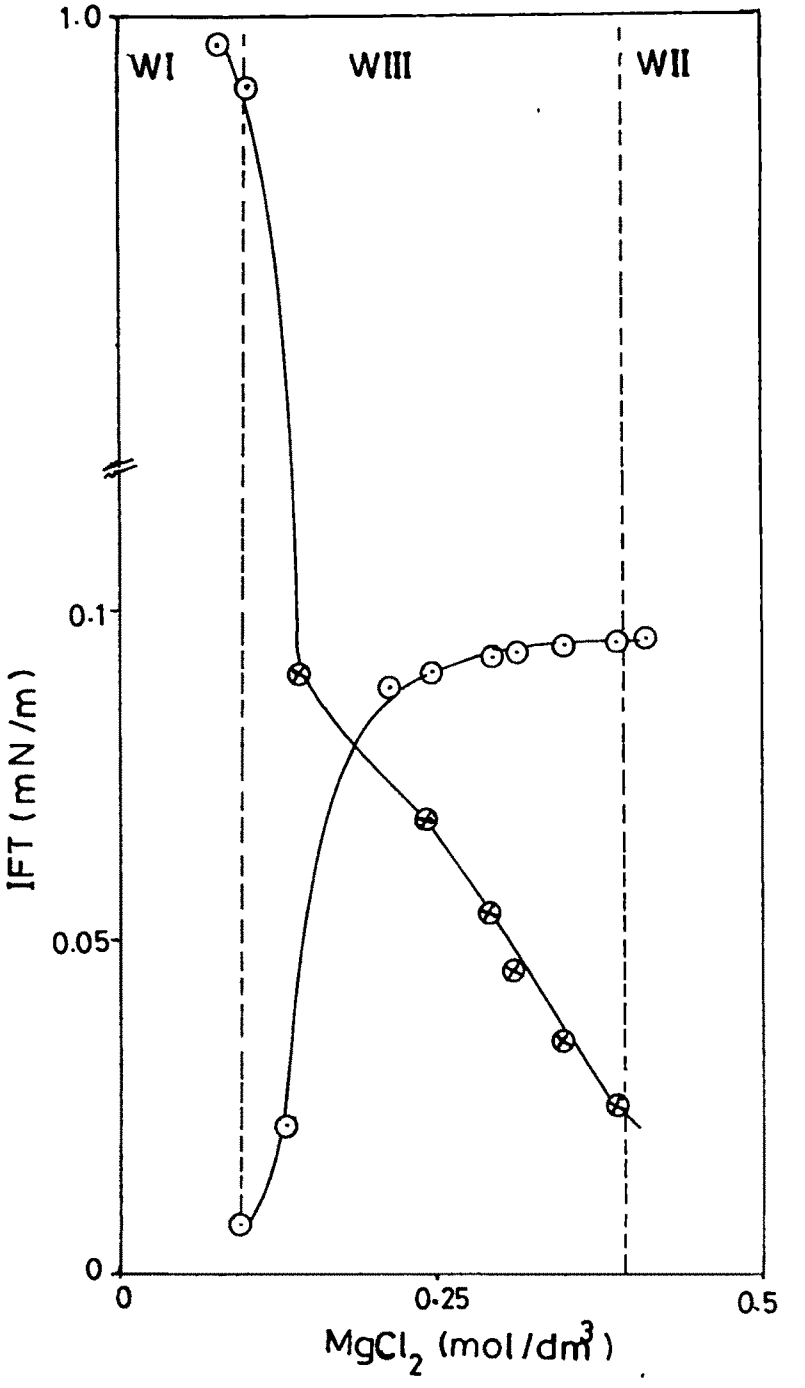

Fig. 3.12 : Plot of variation of interfacial tension (IFT) as a function of concentration of $MgCl_2$ (mol / dm^3) between O/M ⊗, between W/M ⊙.

O = 42.5%; W = 40%; S+CS = 17.5%.

does not have any effect (Table 3.2). This indicates that the anion controls the appearance of the three phase area.

The volume fractions of various layers as a function of concentration of the halides were determined in the absence and also in the presence of 10% PEG. The initiation concentration of the three phase area did not change. We also studied the volume fraction of different layers as a function of the concentration of the electrolytes in the temperature range 30-80°C. Some representative plots are presented in Fig. 3.13. In the presence of n-hexanol, instead of 1-propanol, the transitions are different (WII → WIII → WI). If volumes of oil and water in microemulsion phase and also the volume of microemulsion are represented by V_O, V_W and V_M respectively in a WIII formation, then the solubilization parameter of oil V_O/V_M and that of water V_W/V_M can be plotted as a function of halide concentrations. Some representative plots are shown in Fig. 3.14. The concentration of the halides at which the solubilization parameters are exactly equal is termed optimal salinity (OS). In Table 3.3, the optimal salinity of all systems studied are given. In our earlier studies, we observed both the increase in OS[9] as well as decrease in OS[23] with temperature. In the present system OS remains more or less constant over the temperature range studied. In the presence of the halides, a three phase system appears because of the favourable hydrophilicity and hydrophobicity induced in the surfactant system by the halides. Different halides effect the hydrophil lipophil balance of the surfactant system differently and it is the halide ions which effect this balance more than the alkali metal ions. When the interfacial amphiphile layer becomes closer to the hydrophil lipophil balanced state (not the HLB number which is the characteristic of the surfactant molecule[31]) in the presence of halides, the WIII region appears. The salinity of the solution effects ionic surfactant microemulsion systems in the same way as the temperature effects the nonionic surfactant systems. We, therefore, suggest that in the presence of 1-propanol the hydrophilicity of the present system attains a magnitude which does not change by the rise in temperature or the addition of any halide and hence the OS values are independent of temperature (Table 3.3). The cosurfactant 1-propanol is partitioned

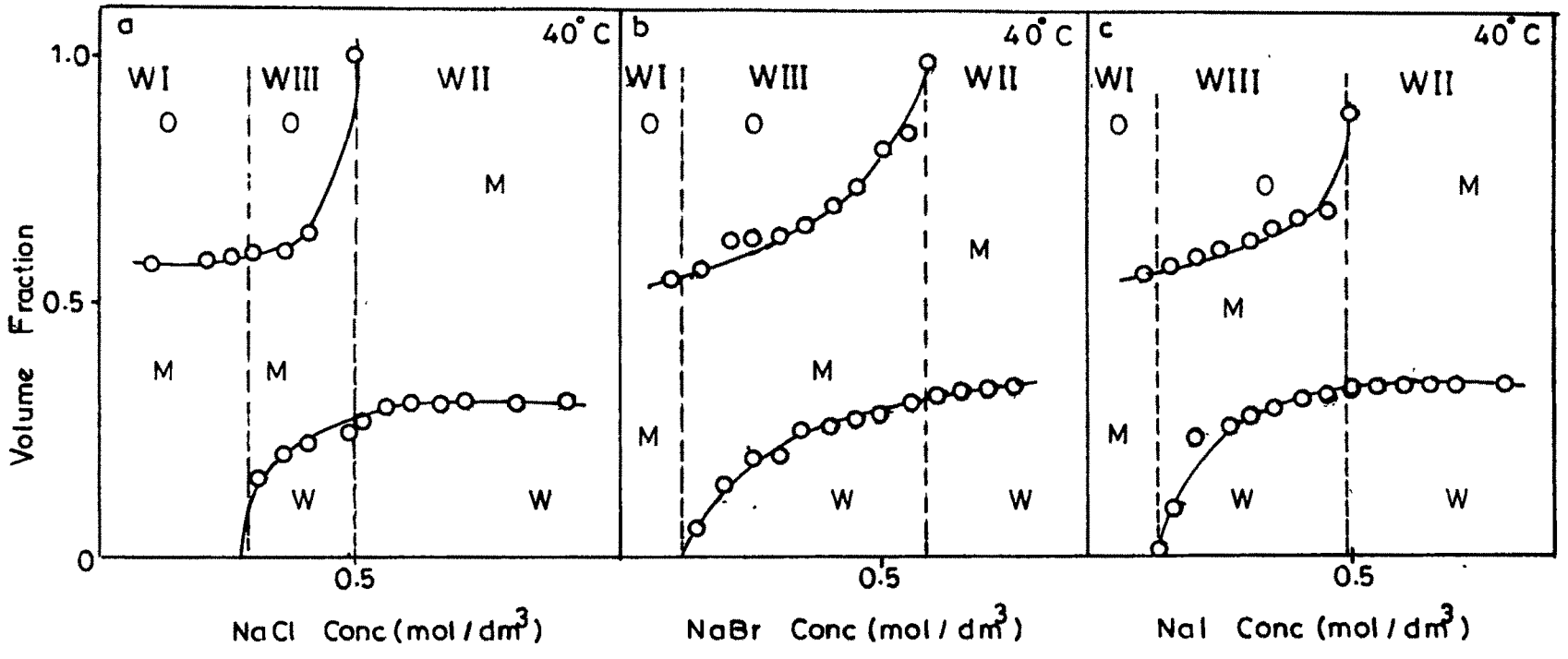

Fig. 3.13 : Representative plots of various volume fractions as a function of concentration of NaCl, NaBr and NaI (mol / dm^3) in absence of (10% w/v) PEG-400 a, b and c at 40°C.

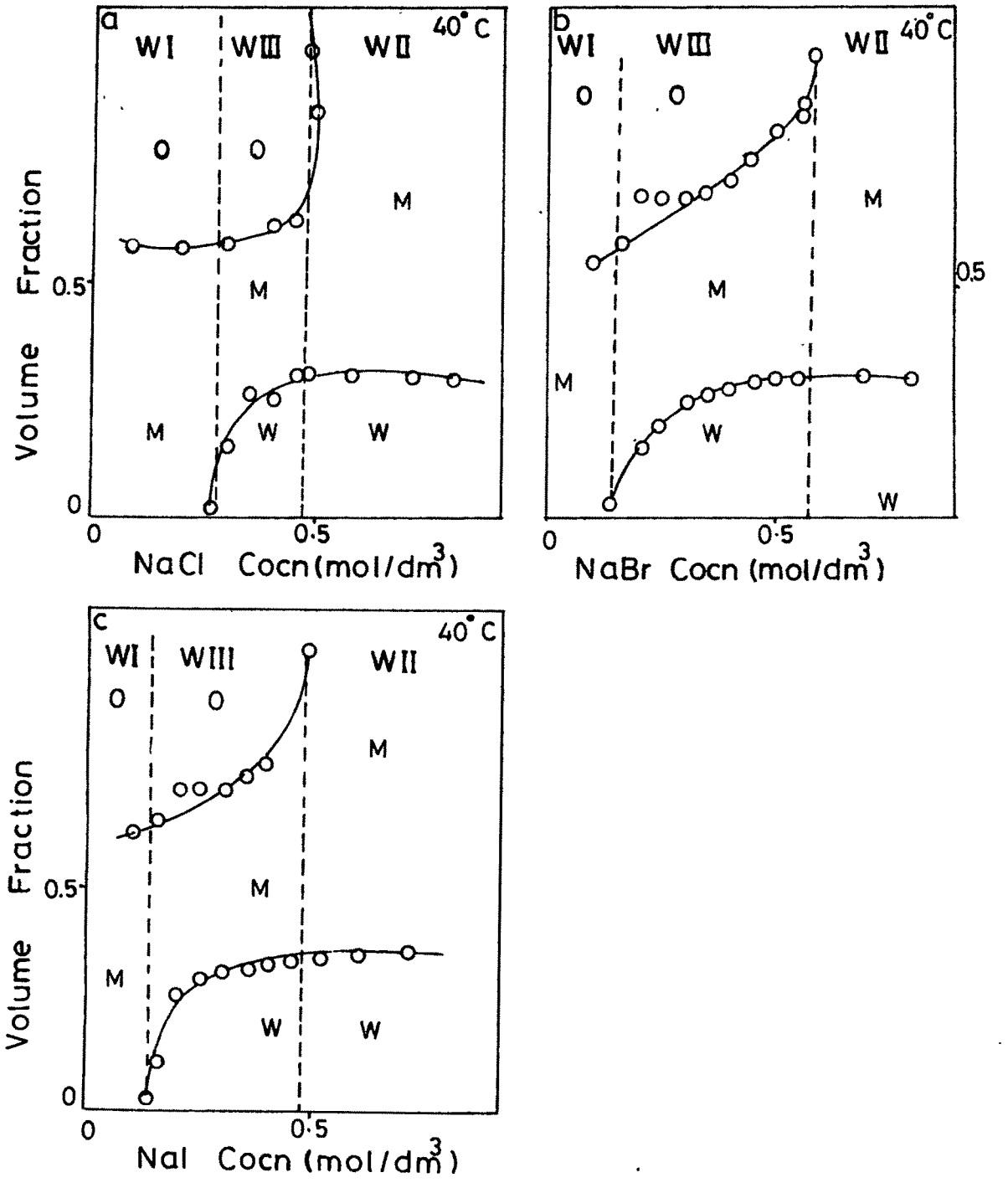

Fig. 3.13 : Representative plots of various volume fractions as a function of concentration of NaCl, NaBr and NaI (mol / dm^3) in presence of (10% w/v) PEG-400a, b and c at 40°C.

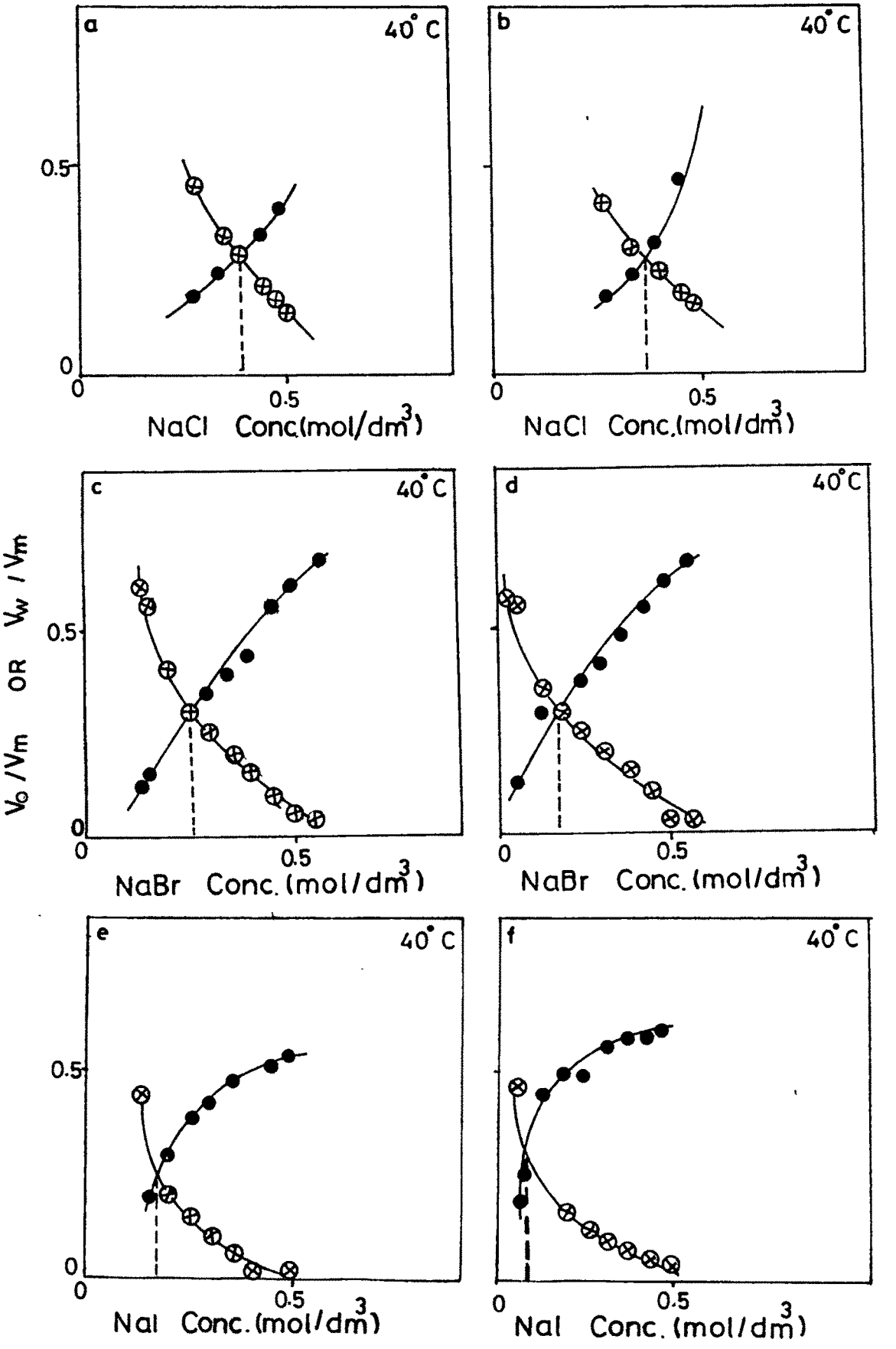

3.14 : Plot of Vo/Vm (●) and Vw/Vm ⊗ as a function of NaCl, NaBr and NaI concentration in (mol / dm^3) .40°C a, c and e without PEG-400 b, d and f are with 10% (w/v) PEG-

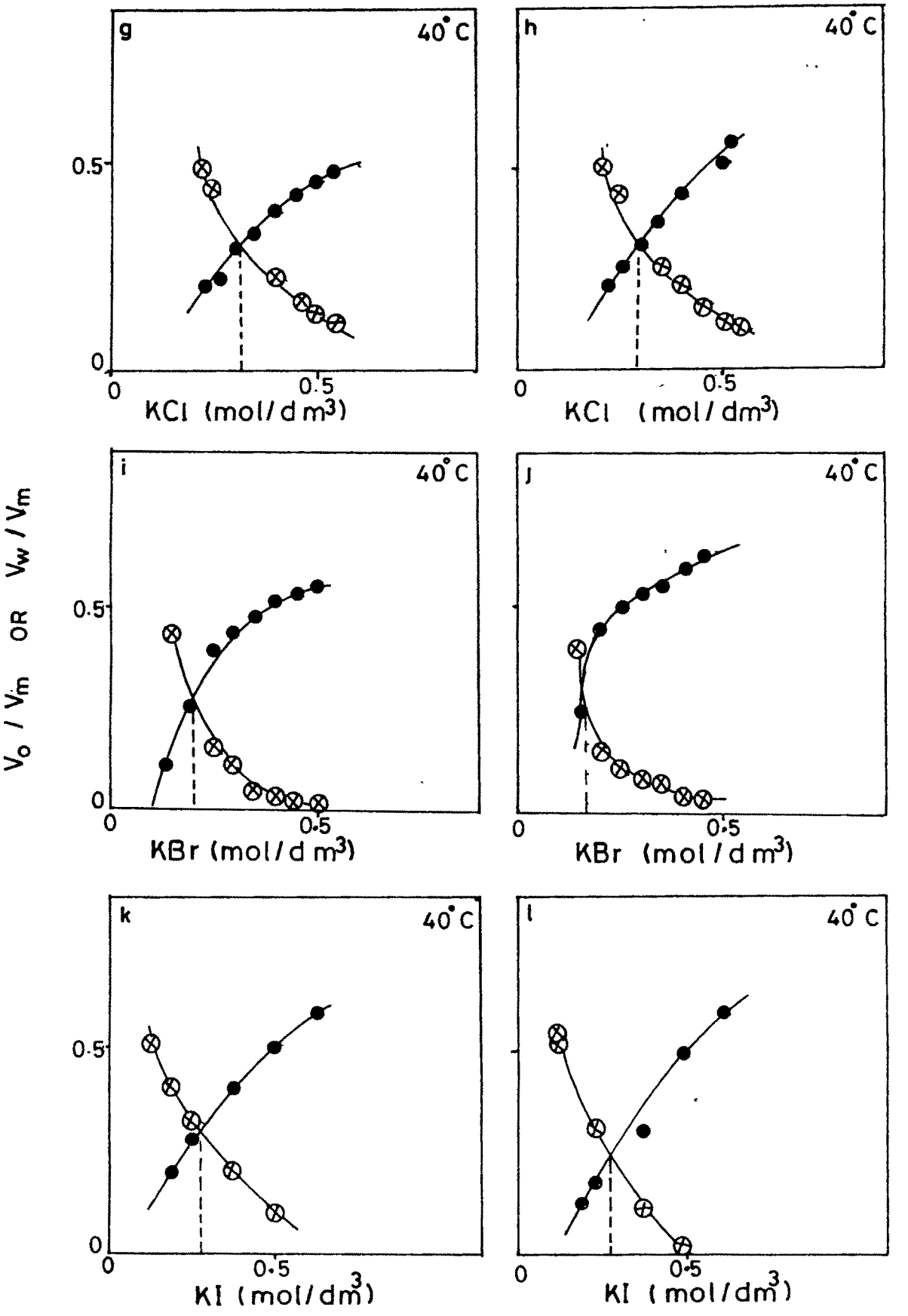

Fig. 3.14 : Plot of Vo/Vm (●) and Vw/Vm ⊗ as a function of KCl, KBr and KI concentration in (mol / dm^3) at 40°C g, i and k without PEG-400 h, j and l are with 10% (w/v) PEG- 400

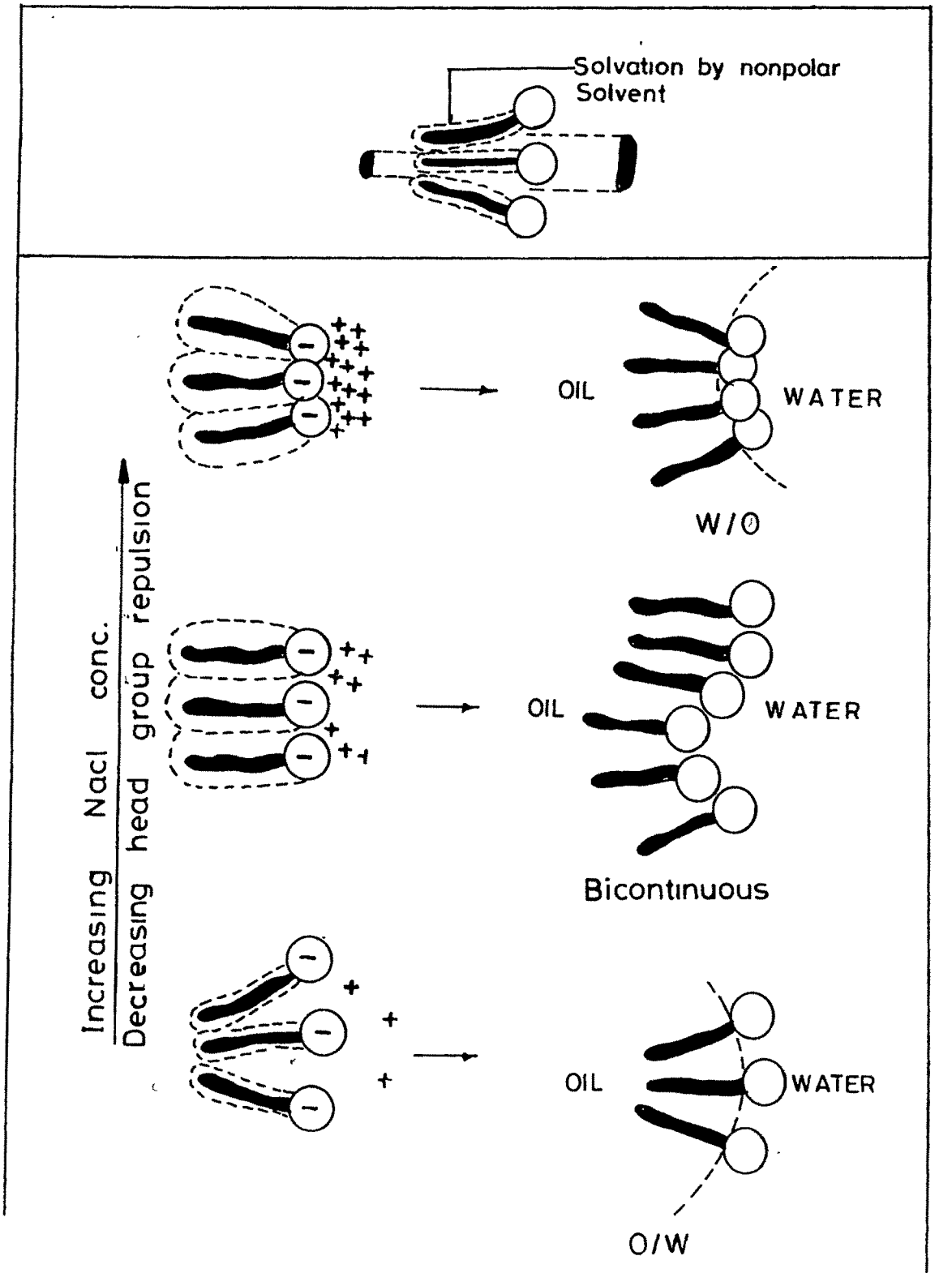

Fig. 3.15 : Representation of the change of oil / water to bicontinuous to water / oil microemulsion. With increasing NaCl (salt) concentration or decreasing head group repulsion. ~~O represents surfactant.

Table 3.2 : The concentration of the electrolytes (molar) at the transition points (WI to WIII) and (WIII to WII) at various temperatures :

WI to WIII					System		WIII to WII				
40°C	50°C	60°C	70°C	80°C			40°C	50°C	60°C	70°C	80°C
0.28	0.28	0.28	0.28	0.28	NaCl	H_2O	0.47	0.47	0.47	0.47	0.47
0.25	0.28	0.28	0.29	0.29	PEG-400	10% w/v	0.47	0.47	0.47	0.46	0.46
0.13	0.13	0.13	0.13	0.13	NaBr	H_2O	0.57	0.57	0.57	0.57	0.57
0.13	0.13	0.13	0.12	0.12	PEG-400	10% w/v	0.57	0.57	0.57	0.55	0.55
0.14	0.14	0.14	0.14	0.14	NaI	H_2O	0.49	0.49	0.49	0.49	0.49
0.14	0.14	0.14	0.13	0.13	PEG-400	10% w/v	0.49	0.49	0.49	0.47	0.47
0.23	0.23	0.23	0.23	0.23	KCl	H_2O	0.54	0.54	0.54	0.48	0.48
0.22	0.22	0.22	0.22	0.22	PEG-400	10% w/v	0.54	0.54	0.54	0.47	0.47
0.14	0.14	0.14	0.14	0.14	KBr	H_2O	0.48	0.48	0.48	0.48	0.48
0.14	0.14	0.14	0.13	0.13	PEG-400	10% w/v	0.48	0.48	0.48	0.46	0.46
0.08	0.08	0.08	0.08	0.08	KI	H_2O	0.27	0.27	0.27	0.26	0.26
0.07	0.07	0.07	0.07	0.07	PEG-400	10% w/v	0.27	0.27	0.27	0.25	0.25

Table 3.3 : The optimal salinity (molar) at various temperatures for the system cyclohexane (42.5%) / CTAB + 1-propanol (17.5%) / X in presence of various electrolytes :

X (40%)	Electrolyte	Temperature (°C)				
		40	50	60	70	80
Water	NaCl	0.39	0.39	0.39	0.38	0.38
10% PEG	NaCl	0.37	0.37	0.37	0.35	0.35
Water	NaBr	0.25	0.25	0.25	0.25	0.25
10% PEG	NaBr	0.25	0.25	0.25	0.25	0.23
Water	NaI	0.17	0.17	0.17	0.17	0.16
10% PEG	NaI	0.16	0.16	0.16	0.15	0.15
Water	KCl	0.32	0.32	0.32	0.30	0.29
10% PEG	KCl	0.30	0.30	0.30	0.28	0.27
Water	KBr	0.20	0.20	0.20	0.15	0.15
10% PEG	KBr	0.15	0.15	0.15	0.15	0.11
Water	KI	0.11	0.11	0.11	0.11	0.10
10% PEG	KI	0.11	0.11	0.11	0.10	0.10

between oil and water. In the Fig. 3.15 a suggested pictorial representation is presented. With the increase in temperature, these bonds break up and the propanol molecules move to the interface. The interface becomes more hydrophilic due to rise in temperature and that is just compensated by the increase in hydrophobicity and hence the hydrophil lipophil balance becomes independent of temperature. The OS therefore remains constant. The effect of PEG-400 was found negligible on optimal salinity values.

The concentration range over which the three phase region exists is independent of temperature for a particular electrolyte. PEG-400 (10% w/v) does not have any effect on this range. In Table 3.3 the concentration of the electrolytes at which transition occurs from WI-WIII and also from WIII-WII are presented. No regularity with respect to the electrolytes was obtained.

The OS value (Table 3.3) were further explored. It was observed that the difference between OS (NaCl) and OS (NaBr) is exactly equal to the difference between OS (KCl) and OS (KBr). Similarly OS (NaCl) - OS (NaI) is exactly equal to the difference in the OS values of KCl and KI. Various other combinations show similar results. In other words the optimal salinity is not the inherent characteristic of the electrolyte but is the characteristic of the ions constituting the electrolyte.

3.3.4 **Electrical conductivity study** :

In Fig. 3 (16-20) the specific conductance (σ) versus volume fraction of water (ϕ_w) are plotted at different temperatures for WIV system at constant S+CS values of 45% and 65% respectively in the mixture. The conductance increases with increase in water concentration (Fig. 3.16). The higher the temperature, the larger the conductance. At higher S+CS concentration of 65%, the magnitude of conductance was much lower (Fig. 3.17). This is because at high S+CS concentration, the water amount is very low and hence the surfactant does not dissociate well. It should also be noted that the percolation is absent in the system. As the water concentration increases, the

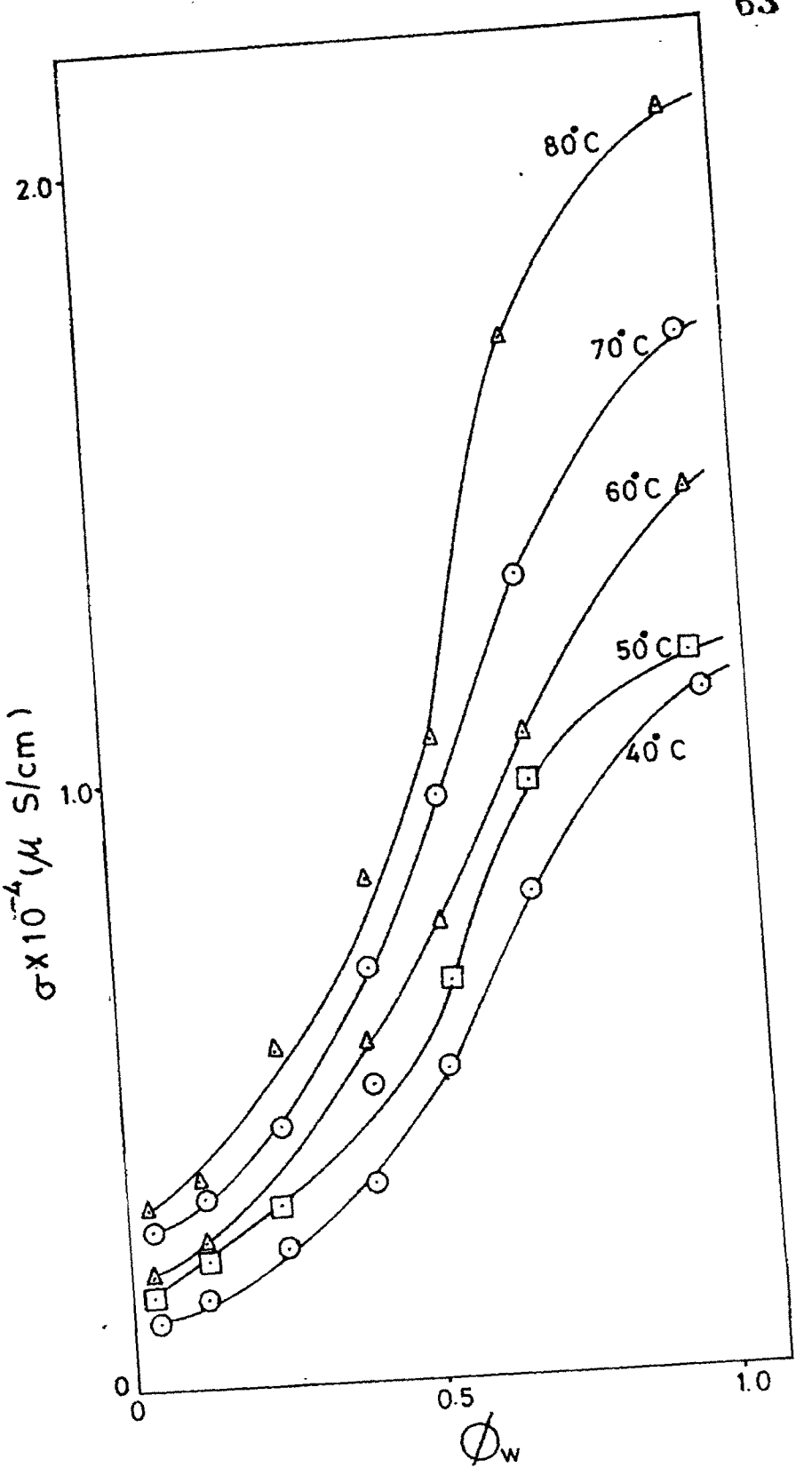

Fig. 3.16 : Plot of specific conductance σ (μs/cm) against volume fraction (ϕ_w) of water at different temperatures S+CS 45%; at 40, 50, 60, 70 and 80°C.

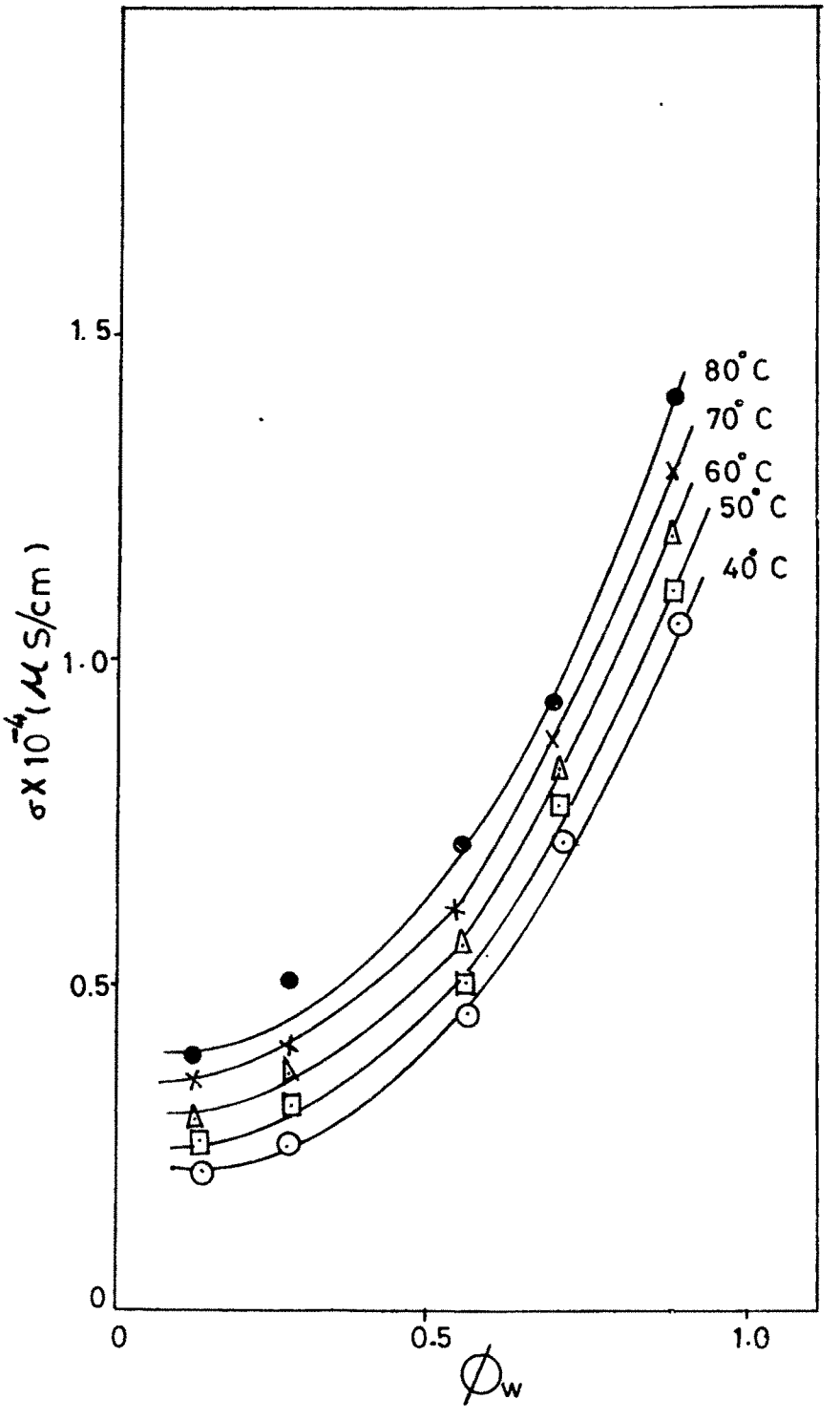

Fig. 3.17 : Plot of specific conductance (σ) (μs/cm) against volume fraction (ϕ_w) of water at different temperature with S+CS (10% w/v) PEG-400 at 40, 50, 60, 70 and 80°C.

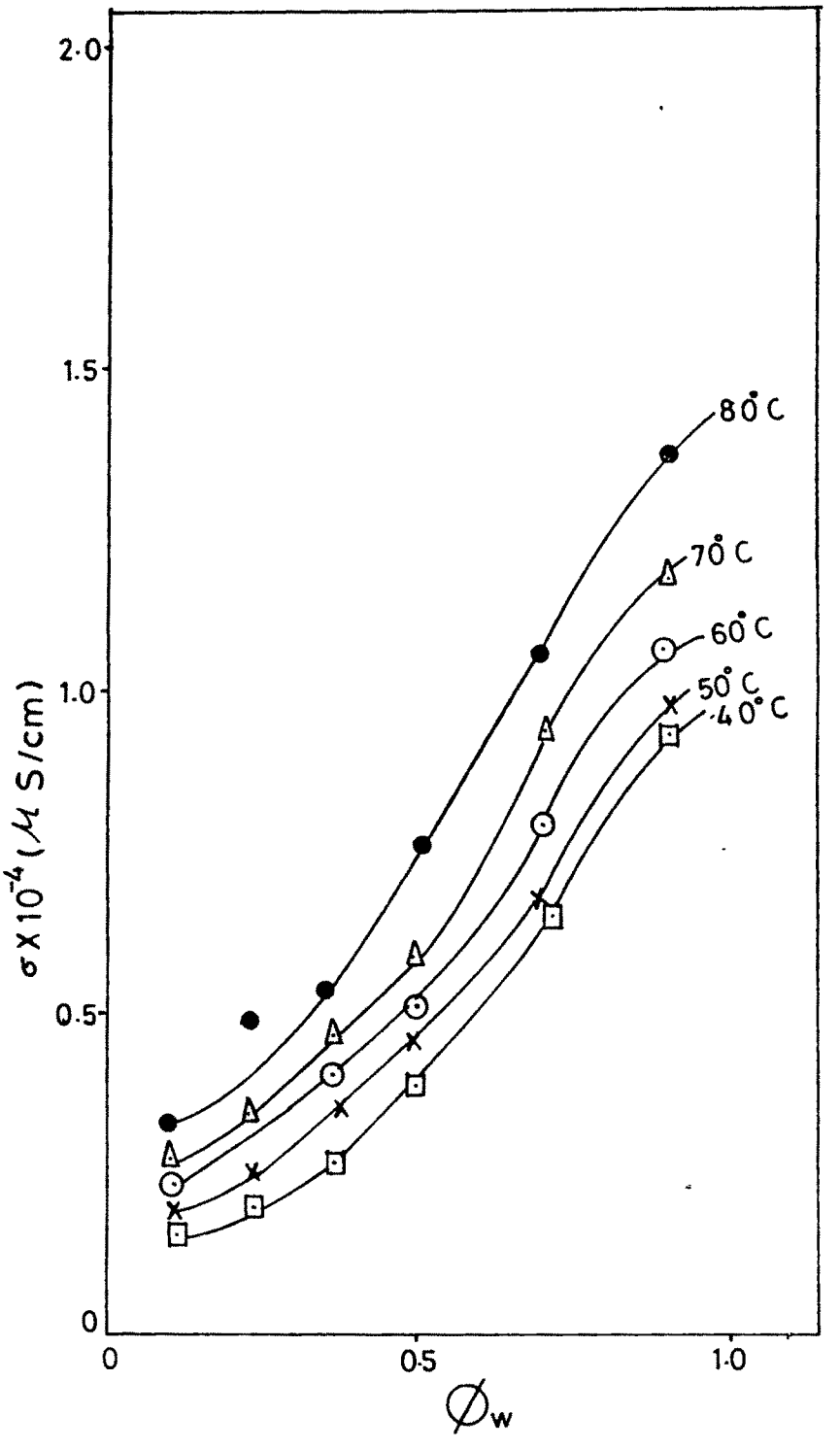

Fig. 3.18 : Plot of specific conductance σ (μs/cm) against volume fraction (ϕ_w) of water at different temperature with S+CS 65% at 40, 50, 60, 70 and 80°C.

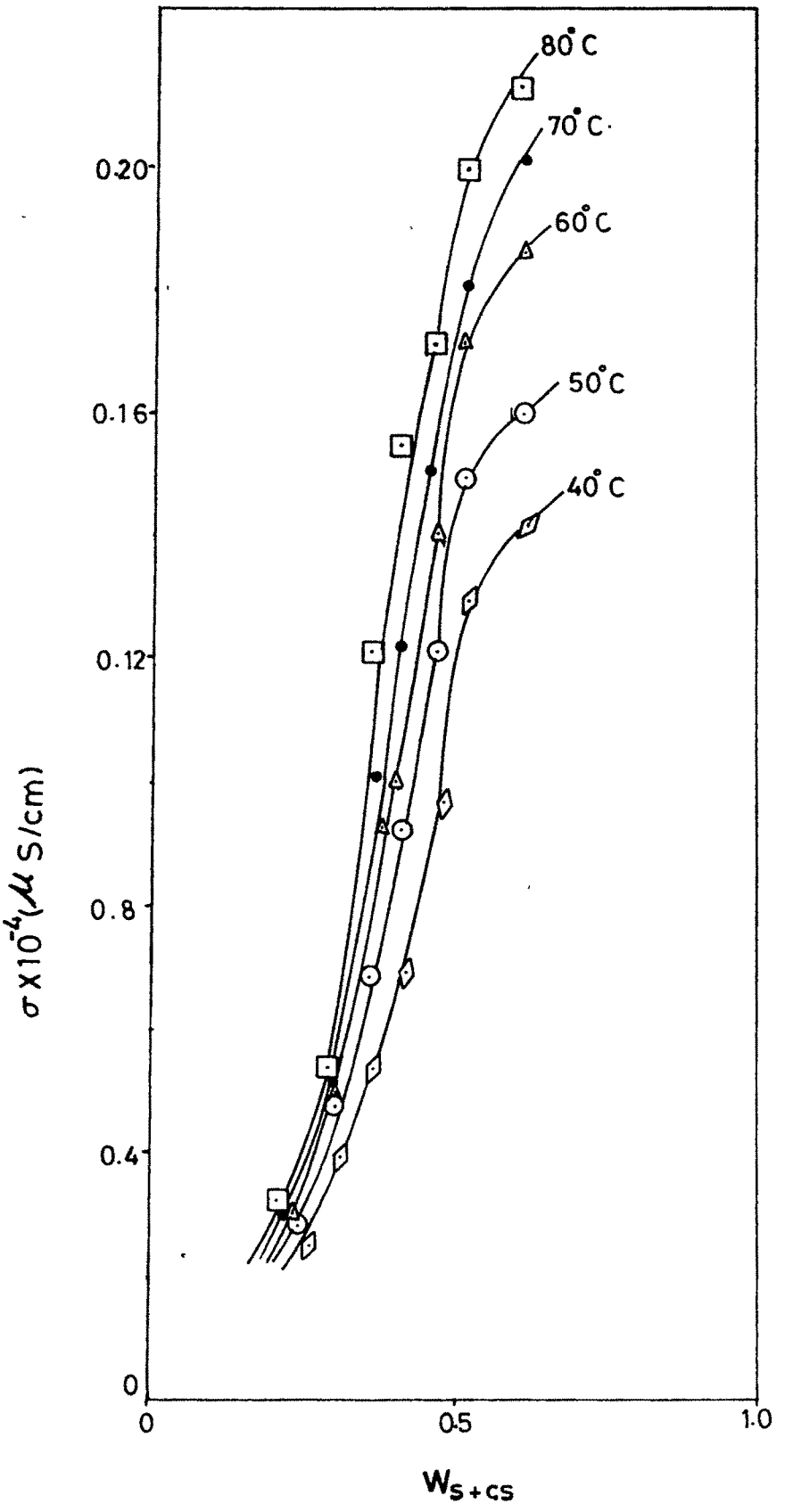

Fig. 3.19 : Plot of specific conductance (σ) (μs/cm) against weight fraction W_{S+CS} at different temperature at constant W = 5% at 40, 50, 60, 70 and 80°C.

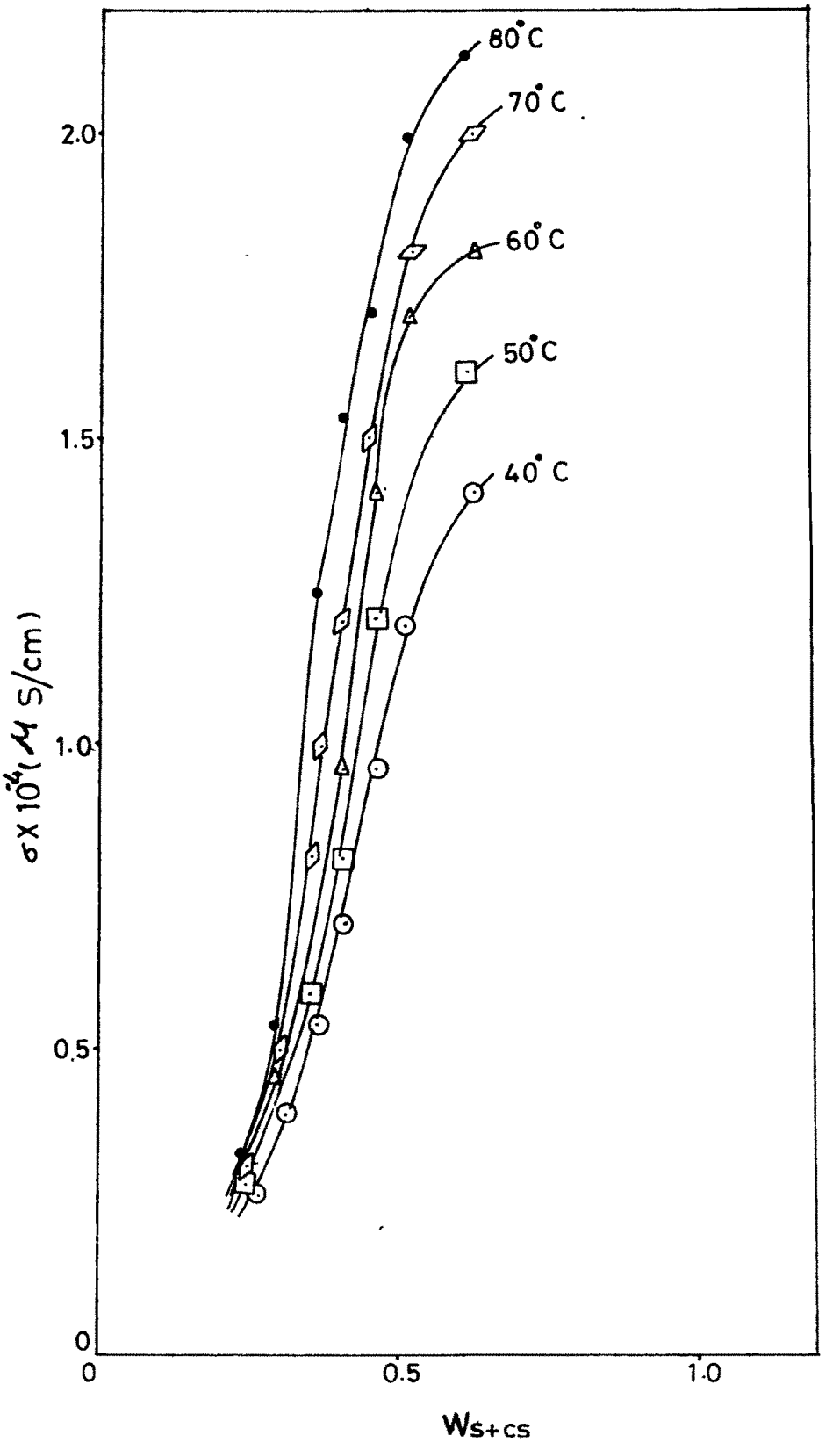

Fig. 3.20 : Plot of specific conductance (σ) (μs/cm) against weight fraction W_{S+CS} at different temperature at constant W = 5%.

surfactant present at the oil-water interface ionises more, thereby increasing the conductance. Hence, 45% S+CS system shows much higher conductance. The presence of PEG decreases the conductance. The presence of PEG means that the amount of water is less and hence less conductance as ionic conductance in PEG is less than that in water.

There are two mechanisms to explain the conductance in a microemulsion system : the hopping[32] and the sticky collision[33]. In the present case, we believe the conductance is due to sticky collision. If hopping was applicable then the conductance should have been much higher. In the present case, both in the presence and absence of PEG, the water channel fusion occurs forming a bigger water channel. Therefore, the conductance slowly increases as ion transport occurs in the water channel. We, therefore, presume that the system is biocontinuous in nature. Ninham et al.[34,35] observed such behaviour in the presence of cationic dodecyl dimethylammonium bromide. It was suggested by Lagourette et al.[14] that the conductance in microemulsion obeys a relation -

$$\sigma \alpha (\phi_w - \phi^p_w)^t$$

where ϕ^p_w is the percolation threshold of the water volume fraction, over which the percolation might be observed. For a biocontinuous system, t has been suggested to be 8/5. Therefore, one can write that $\sigma^{5/8} = A (\phi_w - \phi^p_w)$ where A is a proportionality constant. $\sigma^{5/8}$ versus ϕ_w plots are reasonably linear (Fig. 3.21). From the intercept in the X axis, the ϕ^p_w can be computed and found to have negative value. The structure of microemulsion was assumed to be similar over the oil-water ratio studied[22,37]. The constant A was found to be a function of both PEG concentration and temperature.

3.3.5 Viscosity Study :

In Fig. 3 (22-23), the viscosity versus ϕ_w plots, both in the presence and absence of PEG are shown for systems with S+CS = 45% as well as 65%. Viscosity is a direct function of water concentration. The increase in water concentration increases the water channel volume, a more structured system, and hence viscosity. However, it is

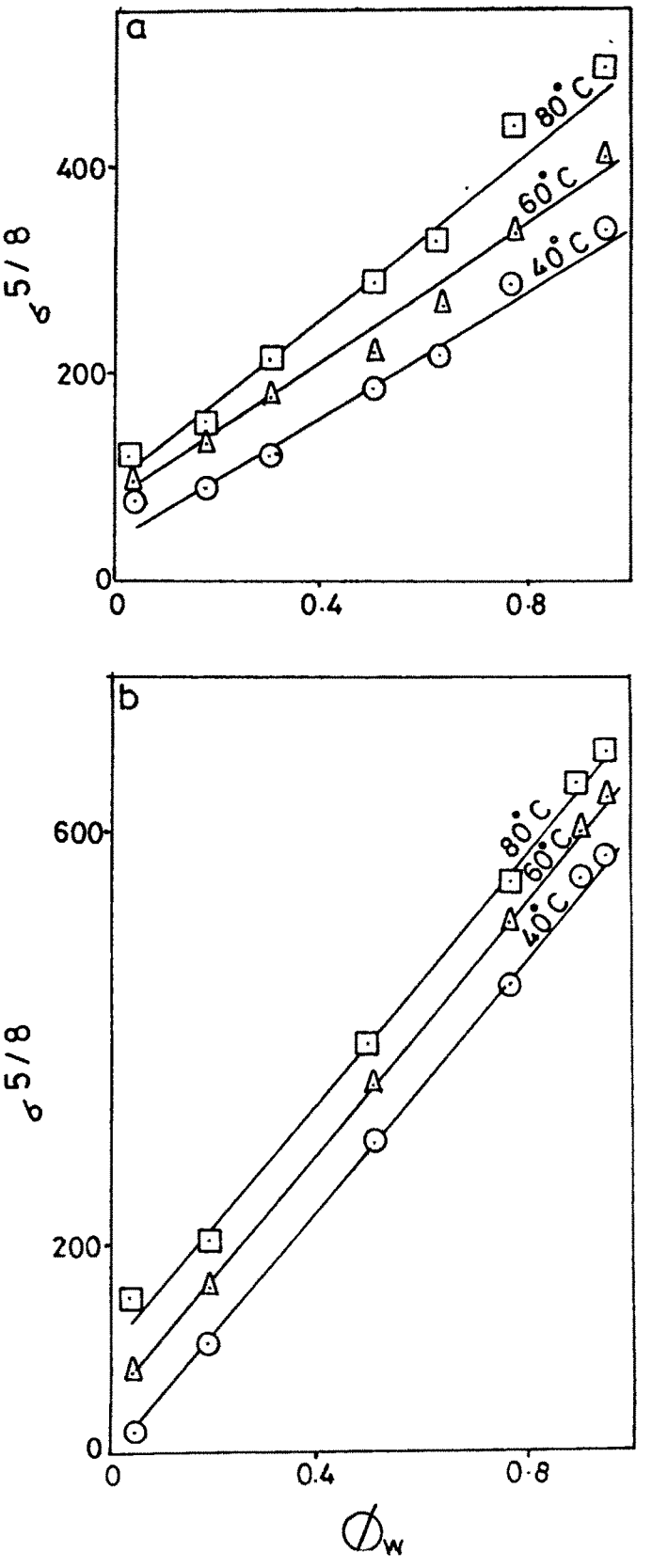

Fig.3.21 : Plot of $\sigma^{5/8}$ against volume fraction of water (ϕ_w), σ is specific conductance (μs/cm) (a) without PEG-400 S+CS 45%; (b) with PEG-400 S+CS 45%; at (O) 40°C, (Δ) 60°C, (□) 80°C.

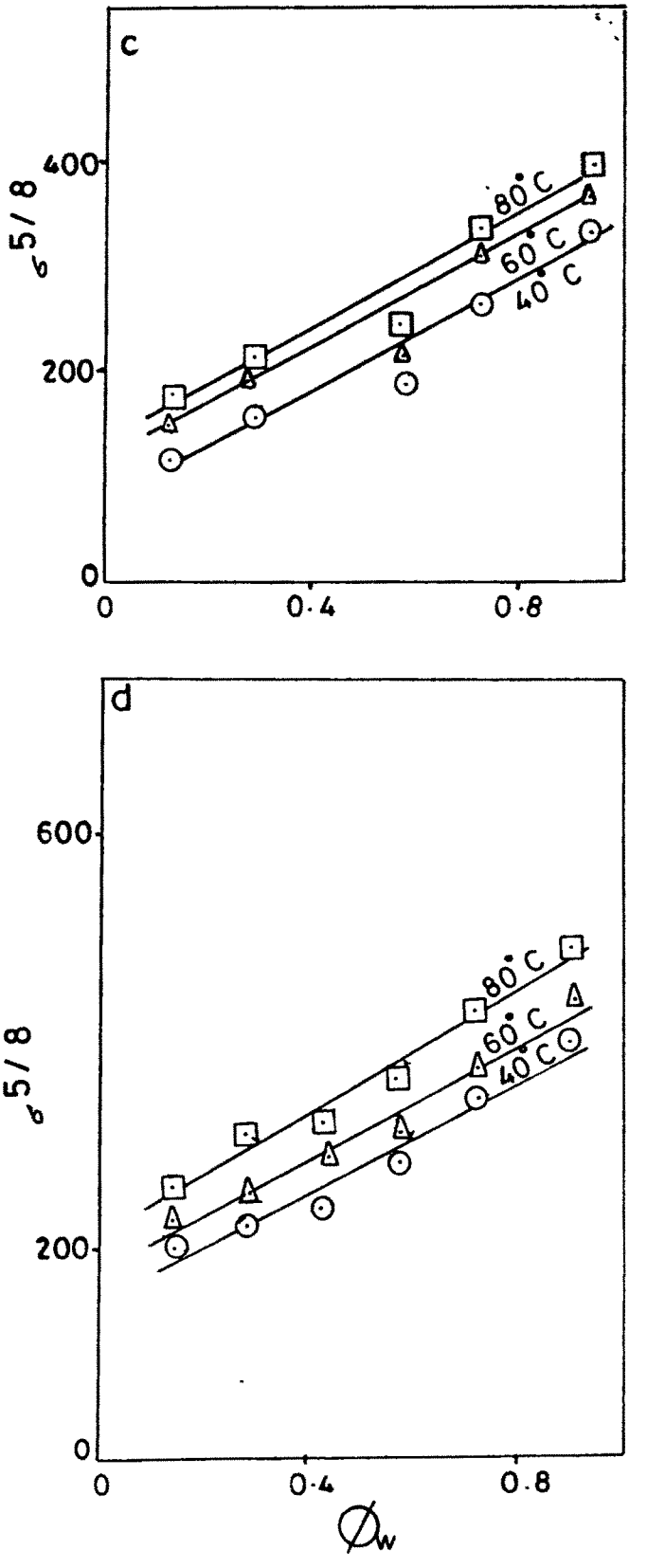

Fig.3.21 : Plot of $\sigma^{5/8}$ against volume fraction of water (ϕ_w), σ is specific conductance (μs/cm) (c) without PEG-400 S+CS 65%; (d) with PEG-400 S+CS 65%; at (O) 40°C, (Δ) 60°C, (□) 80°C.

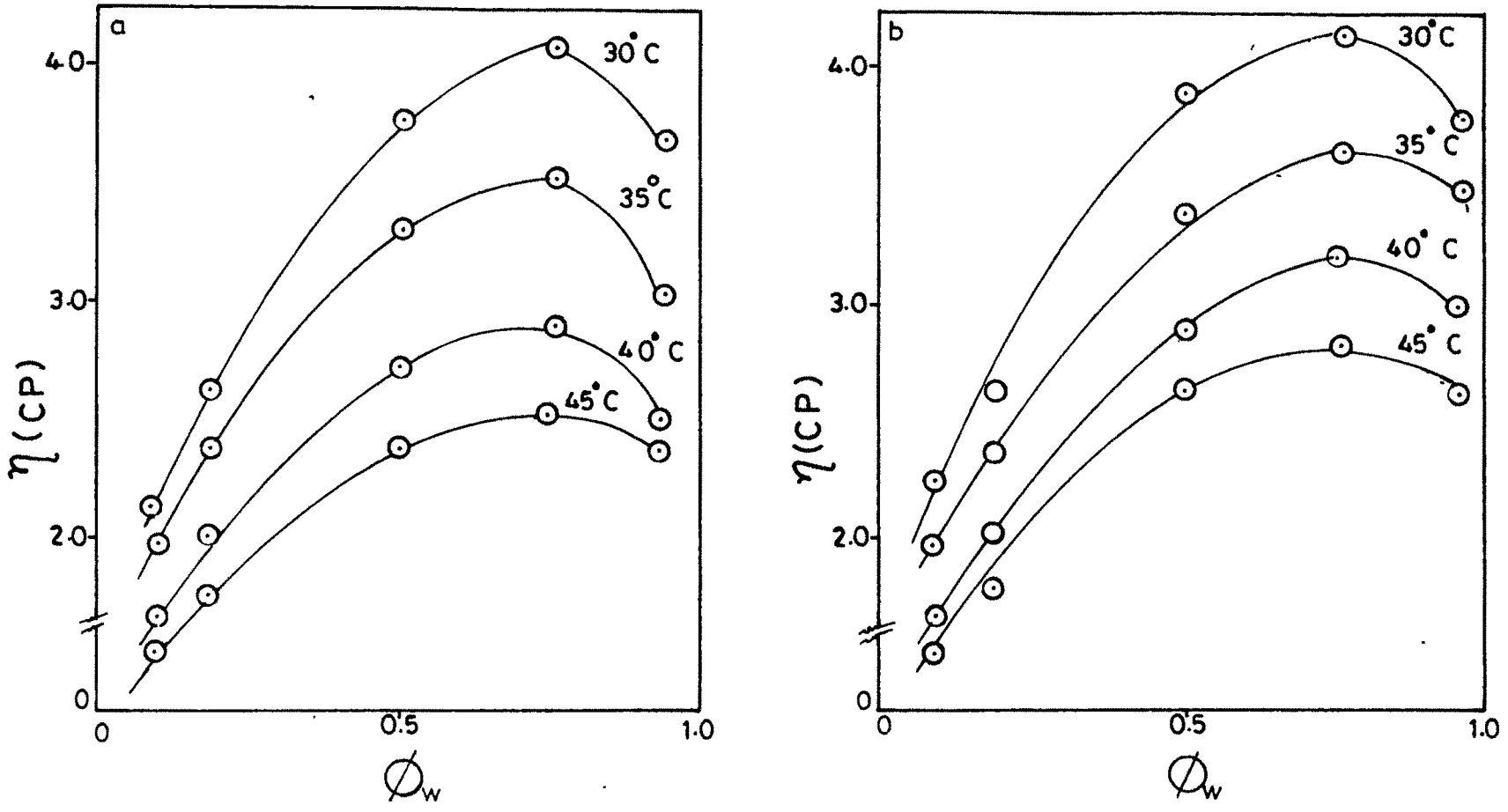

Fig. 3.22 : Plot of viscosity η(CP) vs volume fraction of water (ϕ_w) at various temperatures for different systems; S+CS 45%; a - in absence of PEG-400; b - in presence of 10% (w/v) PEG-400 at 30, 35, 40 and 45°C.

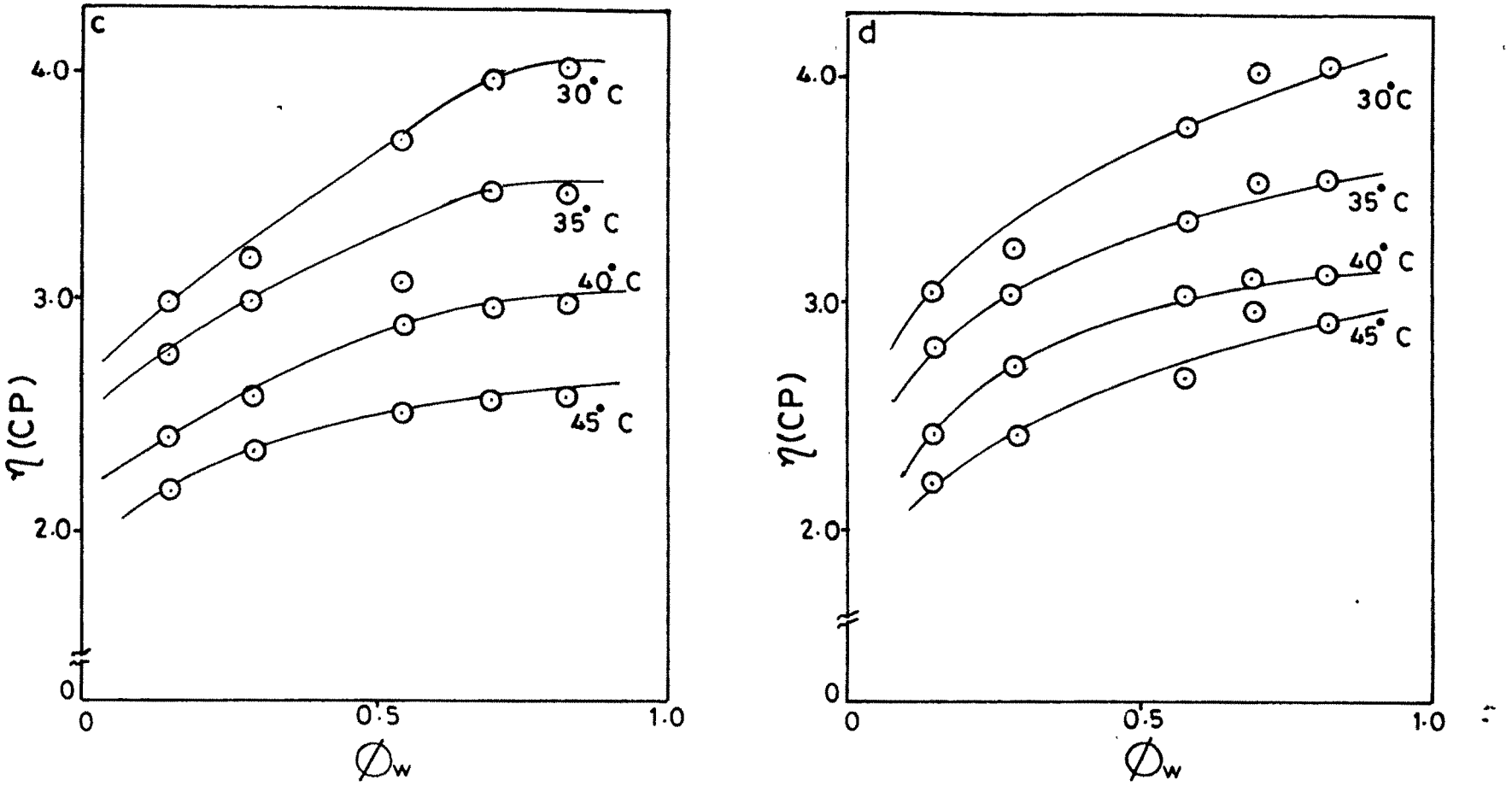

Fig. 3.23 : Plot of viscosity η(CP) vs volume fraction of water (ϕ_w) at various temperatures for different systems. S+CS 65%, (c) in absence of PEG-400, (d) in presence of (10% w/v) PEG-400.

observed that in 45% S+CS, the viscosity decreases after the volume fraction of water reaches ~ 0.8. A maximum is observed around this concentration. This indicates the change in the system from a bicontinuous to O/W regime. However, the viscosity should have been constant rather than showing a maximum. The maximum is observed because of the dilution by further addition of water[22]. In the presence of PEG (10% w/v), the viscosity is higher. This is because PEG-400 is more viscous than water and hence the overall increase in viscosity. Qualitatively though the curves are similar and dilution effect can also be noted.

In 65% S+CS (Fig. 3.23) system, the viscosity is much higher than in the 45% system. However, the increase in viscosity with addition of water is not as high. The dilution effect, though probably present, is not obvious. In the presence of PEG, the viscosity is higher. The dilution effect in this case is not prominent because concentration of surfactant is very high here and the addition of water is used to swell up the water channel - that is more structure formation. At 45% S+CS, the dilution effect is observed because the channels have size constrain and the maximum size is reached at $\phi_w = V_w / (V_w + V_o)$ equal to 0.8 and also due to change in the nature of the regime. It is to be noted that volume of water is much less in the 65% system than in the 45% one for the same ϕ_w equal to 0.8. The viscosity values were used to compute the activation enthalpy of the viscous flow using the Frenkel-Eyring equation[21,38] -

$$\eta = Nh / V \exp (\Delta G^{\neq} / RT)$$

where N, h and V are Avogadro nuber, Plancks constant and molar volume respectively. Therefore, one can write -

$$\ln \eta V / Nh = (\Delta H^{\neq} / RT) - (\Delta S^{\neq} / R)$$

and good linear plots were observed between $\ln \eta V / Nh$ and T^{-1} (Fig. 3.24). The calculated $\Delta H^{\neq}$ values (Table 3.4) are higher in relatively high viscous, more water containing systems than in more oil containing low viscous systems. As the oil concentration decreases, the $\Delta H^{\neq}$ values for the systems with PEG becomes lower

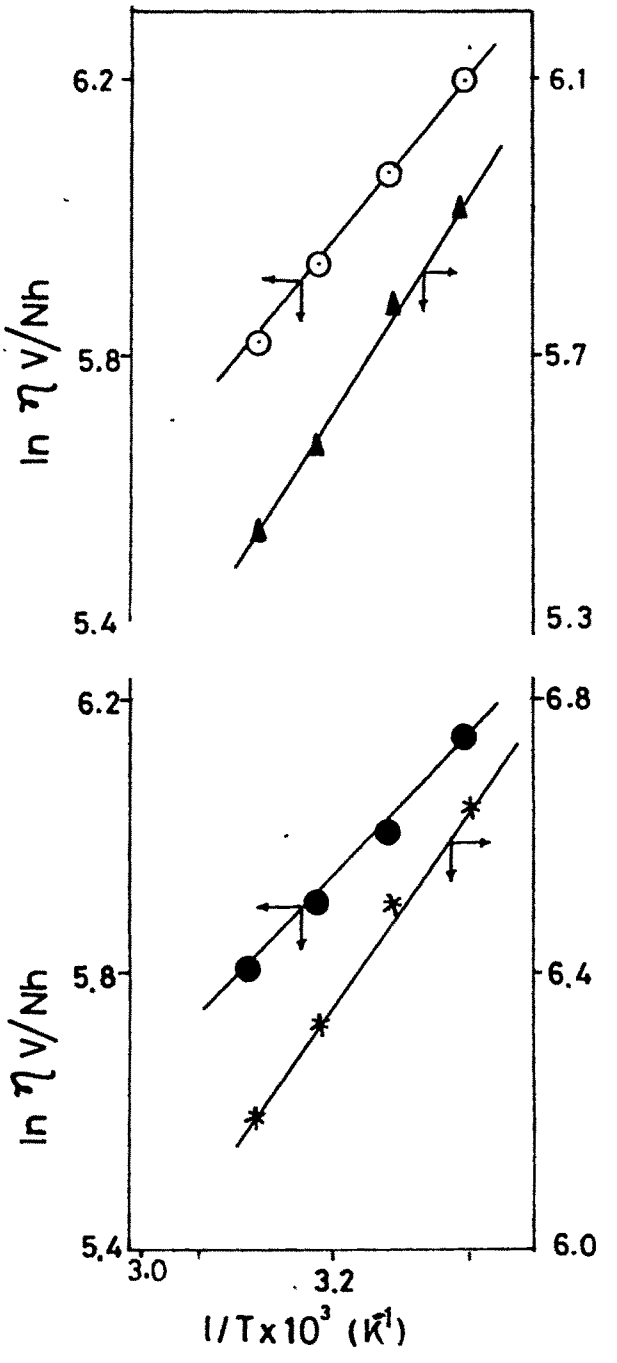

Fig. 3.24 : Representative plots of S+CS : 45% log ηV/Nh Vs T^{-1} for systems with S+CS 45%; and W/O volume ratios (⋄) 10/45; (O) 5/50; (✳) 27.5/27.5; (●) 42.5/12.5.

Table 3.4 : The activation enthalpy $\Delta H^{\neq}$ (kJ/mol) at various oil / water ratios :

System (O/W)	In the absence of PEG	In the presence of 10% PEG
(45% S + CS)		
50/5	17.1	19.5
45/10	19.3	19.7
27.5/27.5	22.5	20.3
12.5/52.5	23.3	22.0
2.5/52.5	25.00	22.9
(65% S + CS)		
30/5	14.8	14.8
25/10	15.4	15.4
15/20	20.0	18.1
10/25	21.4	19.1
2.5/32.5	25.5	20.8

than those without PEG. This is because the rate of variation of ηV with temperature at low oil concentration is, in the presence of PEG, less than in the absence of PEG.

REFERENCES

1) D.J.Cebula, D.Y.Myres and R.H.Ottewill; J. Colloid Polym. Sci., **260**, 96 (1982).
2) P.L.Debruyn, J.Th.G.Overbeek and F.Verhockx; J. Colloid Interface Sci., **127**, 245 (1989).
3) N.Mitra, L.Mukhopadhyay and S.P.Moulik; Indian J. Biochem. Biophys., **31**, 115 (1994).
4) L.Mukhopadhyay, S.Gupta and S.P.Moulik; Indian J. Biochem. Biophys., **32**, 61 (1995).
5) M.J.Suarez and J. Lang; J. Phys. Chem., **99**, 4626 (1995).
6) A.Jada, J.Lang, S.J.Candau and R. Zana; Colloids Surfaces, **38**, 231 (1989).
7) S.J.Candau, E.Hirsch and R.Zana; J. Colloid Interface Sci., **105**, 521 (1985).
8) D.B.Siano and J.Bock; J. Colloids Interface Sci., **90**, 359 (1982).
9) A.C.John and A.K.Rakshit; Colloids Surf., **95A**, 201 (1995).
10) A.P.Holmberg and B.Wesslen; J. Phys. Chem., **66**, 462 (1996).
11) M.J.Suarez, M.Levy and J.Lang; J. Phys. Chem., **97**, 9808 (1993).
12) K.Shinoda, Y.Shibata and B.Lindman; Langmuir, **9**, 1254 (1993).
13) D.Papautsi, P.Lianos and W.Brown; Langmuir, **10**, 3402 (1994).
14) P.G.Nilson and B.Lindman; J. Phys. Chem., **87**, 4756 (1983).
15) S.P.Moulik, S.Gupta and A.R.Das; Can. J. Chem., **67**, 356 (1989).
16) J.Th.G,Overbeek, P.L.deBruyn and F.Verhockx, In Surfactants, edited by Th.F.Tadros, Academic Press, London (1984).
17) J.H.Clint; In Surfactant Aggregation, Blackie, Glasgow (1992).
18) A.Jada, J.Lang and R.Zana; J. Phys. Chem., **94**, 381 (1990).
19) R.Zana, J.Lang and D.Canet; J. Phys. Chem., **95**, 3364 (1991).
20) E.B.Abuin, M.A.Rubio and E.A.Lissi; J. Colloid Interface Sci., **158**, 129 (1993).
21) G.Wang and G.Olofsson; J. Phys. Chem., **99**, 5588 (1995).
22) a) A.C.John and A.K.Rakshit; J. Colloid Interface Sci., **156**, 202 (1993).

b) "Vogel's" Textbook of Practical Organic Chemistry. Longmans, Green, New York, 1978.

23) A.C.John and A.K.Rakshit; Langmuir, **10**, 2084 (1994).

24) S.Ajith and A.K.Rakshit; J. Phys. Chem., **99**, 14778 (1995).

25) S.Ajith and A.K.Rakshit; Langmuir, **11**, 1122 (1995).

26) S.Ajith, A.C.John and A.K.Rakshit; Pure Appl. Chem., **66**, 509 (1994).

27) Vogel's Textbook of Practical Organic Chemistry, Longman, London, (1978).

28) S.Ajith and A.K.Rakshit; J. Surf. Sci. Tech., **8**, 137 (1992).

29) P.Kar and S.P.Moulik; Indian J. Chem., **34A**, 700 (1995).

30) J.E.Puig, D.L.Nemker, A.Gupta, H.T.Davis and L.E.Scriven; J. Phys. Chem., **91**, 1137 (1987).

31) M.J.Vold; J. Colloid Interface Sci., **29**, 181 (1969).

32) R.Hilfiker, H.F.Eicke, S.Geiga and G.Furler; J. Colloid Interface Sci., **105**, 378 (1985).

33) A.Jada, J.Lang and R.Zana; J. Phys. Chem., **93**, 10 (1989).

34) S.J.Chen, D.F.Evans and B.W.Ninham; J. Phys. Chem., **88**, 1631 (1980).

35) S.T.Hyde, B.W.Ninham and T.Zamb; J. Phys. Chem., **93**, 1464 (1989).

36) B.Lagourette, J.Peyrelearse, C.Boned and M.Clausse; Nature, **281**, 60 (1979).

37) E.I.Tessy and A.K.Rakshit; Bull. Chem. Soc. Japan, **68**, 2137 (1995).

38) W.J.Moore; Physical Chemistry, Prentice Hall, Endewood, Clifts, N.J. (1996).